The decay of isotropic magnetohydrodynamics turbulence and the effects of cross-helicity

Antoine Briard, Thomas Gomez

The decay of isotropic magnetohydrodynamics turbulence and the effects of cross-helicity

Antoine Briard[1,2,†] **and Thomas Gomez**[3]

[1]∂'Alembert, CNRS UMR 7190, 4 Place Jussieu, F-75252 Paris CEDEX 5, France
[2]Aix Marseille Université, CNRS, Centrale Marseille, M2P2 UMR 7340, 13451 Marseille, France
[3]USTL, LML, F-59650 Villeneuve d'Ascq, France

Decaying homogeneous and isotropic magnetohydrodynamics (MHD) turbulence is investigated numerically at large Reynolds numbers thanks to the eddy-damped quasi-normal Markovian (EDQNM) approximation. Without any background mean magnetic field, the total energy spectrum E scales as $k^{-3/2}$ in the inertial range as a consequence of the modelling. Moreover, the total energy is shown, both analytically and numerically, to decay at the same rate as kinetic energy in hydrodynamic isotropic turbulence: this differs from a previous prediction, and thus physical arguments are proposed to reconcile both results. Afterwards, the MHD turbulence is made imbalanced by an initial non-zero cross-helicity. A spectral modelling is developed for the velocity–magnetic correlation in a general homogeneous framework, which reveals that cross-helicity can contain subtle anisotropic effects. In the inertial range, as the Reynolds number increases, the slope of the cross-helical spectrum becomes closer to $k^{-5/3}$ than k^{-2}. Furthermore, the Elsässer spectra deviate from $k^{-3/2}$ with cross-helicity at large Reynolds numbers. Regarding the pressure spectrum E_P, its kinetic and magnetic parts are found to scale with k^{-2} in the inertial range, whereas the part due to cross-helicity rather scales in $k^{-7/3}$. Finally, the two 4/3rd laws for the total energy and cross-helicity are assessed numerically at large Reynolds numbers.

Key words: plasma dynamics, plasma nonlinear phenomena, plasma simulation

1. Introduction

For a large variety of astrophysical and geophysical turbulent flows such as in the interstellar medium and stellar winds, the fluid can be conductive, thus creating a complex interplay between the magnetic and velocity fields. The dynamics of both fields can be significantly altered depending on the forcing mechanisms applied or not to the turbulent flow. A relevant framework to model such configurations is magnetohydrodynamics (MHD) turbulence, where the two fields are strongly coupled through the Lorentz force. The MHD framework has been considered multiple times to describe low frequency solar wind dynamics for instance (Galtier 2009; Boldyrev *et al.* 2011).

† Email address for correspondence: antoine.briard92@gmail.com

In the last decades, multiple configurations have been studied, from isotropic MHD turbulence (IMHDT) (Pouquet, Frisch & Léorat 1976; Müller & Biskamp 2000; Müller & Grappin 2004; Carati *et al.* 2006; Yoshimatsu 2012) to strong MHD where a mean magnetic field renders the flow highly anisotropic (Müller, Biskamp & Grappin 2003; Müller & Grappin 2005; Mason, Cattaneo & Boldyrev 2008; Perez & Boldyrev 2009; Boldyrev *et al.* 2011; Perez *et al.* 2012), through weak MHD where the flow tends to be two-dimensional with a dynamics mainly governed by waves rather than inertial effects (Galtier, Pouquet & Mangeney 2005; Boldyrev & Perez 2009; Galtier 2009) and quasi-static MHD where only the equation for the velocity field is considered, with a ohmic term (Favier *et al.* 2011). Obviously, the previous list is not exhaustive and several other frameworks exist: see Biskamp (2003), Galtier (2016) for a review. It appears than even in the simplest case, namely IMHDT without kinetic and magnetic helicities or a mean magnetic field, two different inertial scalings are found for the spectrum $E(k, t)$ of the total energy: the $k^{-3/2}$ scaling following the phenomenology by Iroshnikov (1964), Kraichnan (1965), hereafter IK; and the hydrodynamic Kolmogorov (1941) phenomenology yielding a $k^{-5/3}$ inertial scaling. This discrepancy is an illustration of the complexity of MHD turbulence, even in an apparently simple framework: it seems that in some of the direct numerical simulations (DNS) dealing with fully isotropic MHD, sometimes the Reynolds numbers is not large enough so that the $k^{-3/2}$ and $k^{-5/3}$ inertial scalings can be hardly distinguished.

A good way to get rid of the Reynolds number limitation could be to use spectral models, such as the eddy-damped quasi-normal Markovian (EDQNM) approximation (Orszag 1970). Using an earlier fundamental study (Kraichnan & Nagarajan 1967), this closure was further extended from hydrodynamics turbulence to isotropic helical MHD by Pouquet *et al.* (1976): in the latter work, which also investigates the effect of kinetic helicity and magnetic helicity, the IK scaling $E \sim k^{-3/2}$ is obtained as a consequence of the modelling choice, along with the inverse cascade of magnetic helicity in k^{-2}, a feature which will not be addressed here.

Note that both the Iroshnikov (1964) and Kraichnan (1965) approaches yield the $k^{-3/2}$ inertial scaling, but it is worth recalling that they use very different arguments. For the former, a mean magnetic field $\boldsymbol{B}^0$ is considered, thus it is essentially an anisotropic configuration. Whereas for the latter, no external magnetic field is present, and it is considered that at each scale λ, the magnetic fluctuations of larger scales $l \geqslant \lambda$ can be seen as a local mean magnetic field. Both methods provide the inertial $k^{-3/2}$ scaling but are fundamentally different. Hence, the vision of Iroshnikov (1964) may be compatible with DNS results in which $E \sim k_{\perp}^{-3/2}$ (Müller & Grappin 2005; Boldyrev 2006; Mason *et al.* 2008; Perez & Boldyrev 2009; Boldyrev *et al.* 2011; Perez *et al.* 2012), where $k_{\perp}$ is the component of the wavevector $\boldsymbol{k}$ perpendicular to the imposed mean magnetic field. At variance with this $k_{\perp}^{-3/2}$ scaling, Goldreich & Sridhar (1995) predicts $k_{\perp}^{-5/3}$, and there are arguments and simulations in favour of this scaling too (Beresnyak 2011, 2014).

Therefore, two questions arise from these considerations. What is the inertial scaling of E in terms of $k_{\perp}$ in a anisotropic configuration? And in terms of k in the isotropic case? Even if the former is of great interest nowadays, studying isotropic MHD remains important and relevant as indicated by Mininni & Pouquet (2007), namely: 'in the absence of $\boldsymbol{B}^0$ and for isotropic initial conditions, one may assume that isotropy is still preserved in the large and intermediate scales'. In addition for IMHDT, it has been shown (i) in Lee *et al.* (2010) that the inertial scaling of E strongly depends at short times on initial parameters; and (ii) in Alexakis (2013), with non-zero magnetic

helicity, that with distinct helical forcing terms for the velocity and magnetic fields of various intensities, the resulting kinetic energy spectrum scales more like $k^{-3/2}$ and the magnetic energy spectrum more like $k^{-5/3}$. These two examples further illustrate the complexity of IMHDT and that there are still open questions and mechanisms to be understood. This is why in the present work we study isotropic MHD with EDQNM, without mean magnetic field, to analyse different topics, such as the decay of the total energy, whose prediction is a fundamental question. The deep understanding of isotropic MHD is a necessary first step toward the modelling of strong MHD, where a three-dimensional EDQNM model in terms of $\boldsymbol{k}$ should be analytically derived, analogously to what exists for rotation (Cambon & Jacquin 1989; Cambon, Mansour & Godeferd 1997), and this will be reported elsewhere.

As mentioned above, the decay of the total energy K deserves some attention. Indeed, its prediction remains quite controversial: several decay rates are proposed with no clear dependence on initial conditions, such as the infrared slope σ of the spectrum at large scales $E(k \to 0) \sim k^\sigma$, except the work of Galtier, Politano & Pouquet (1997) which will be discussed in more detail later. Yet, the total energy K, defined as the sum of the kinetic energy K_V and the magnetic energy K_B, is an inviscid invariant of MHD turbulence and as such deserves great theoretical interest. If one compares the number of papers dedicated to the decay of kinetic energy in hydrodynamics turbulence with the ones dedicated to the decay of total energy in MHD turbulence, the difference is striking. Using EDQNM, we aim at deriving a theoretical prediction for the decay of K at large Reynolds numbers, similarly to what was recently done for the helicity and the passive scalar variance in homogeneous isotropic turbulence (HIT) (Briard *et al.* 2015; Briard & Gomez 2017).

Moreover, EDQNM permits to analyse in a simple way pressure spectra: in the framework of HIT and starting from the Poisson equation, it is possible to express the pressure spectrum as a function of the kinetic energy spectra (Lesieur, Ossia & Metais 1999; Meldi & Sagaut 2013*b*). Here for MHD turbulence, there is an additional contribution of the magnetic field to the Poisson equation, coming from the Laplace force. Thus, it is proposed to study the respective contributions of the kinetic and magnetic fields to the total pressure spectrum.

In addition to magnetic helicity (not studied here) and total energy, MHD turbulence has a third inviscid invariant, namely cross-helicity, which is the scalar product of the fluctuating velocity and magnetic fields. The first analytical considerations about the spectral modelling of cross-helicity date back to Frisch *et al.* (1975). Later, simplified EDQNM equations were used by Grappin *et al.* (1982), Grappin, Pouquet & Léorat (1983) to investigate the influence of cross-helicity on the kinetic and magnetic energy spectra. The main hypothesis in these two references, on top of the EDQNM procedure, was to consider equipartition between kinetic and magnetic energies, by assuming the presence of a mean magnetic field with random orientation, so that the flow remained statistically isotropic instead of axisymmetric. Thus, it appears that high Reynolds numbers simulations of the full EDQNM equations for MHD with cross-helicity were not presented, even though the interest in the cross-helicity increased in the past years (Chandran 2008; Matthaeus *et al.* 2008; Beresnyak & Lazarian 2008; Perez & Boldyrev 2009; Boldyrev *et al.* 2011). As said earlier, we choose to address isotropic MHD turbulence here, without a background mean magnetic field, to further understand the interactions between the cross-correlation and the kinetic and magnetic fields, and to better disentangle strong anisotropic effects from intrinsic properties of the velocity–magnetic correlation.

The manuscript is organized as follows. In §2, the main equations of MHD are recalled, and the EDQNM formalism for the kinetic, magnetic and cross-helical fields

is presented. Then, in §3, balanced isotropic MHD is considered, with zero cross-correlation: first, inertial scalings of the kinetic, magnetic and residual spectra are addressed, along with some discussion about nonlinear transfers. Then, the decay of the total energy is investigated, and theoretical decay exponents are proposed and assessed numerically. Afterwards, in §4, the emphasis is put on the modelling of the cross-helicity, its impact on spectral scalings and short-time dynamics; pressure spectra are also analysed. Section 5 is dedicated to statistics in physical space, with in particular the numerical assessment of the 4/3rd laws for total energy and cross-helicity. Conclusions and perspectives are gathered in the final section.

2. Spectral evolution equations for isotropic MHD turbulence

In this part, the evolution equations of the velocity and magnetic fields are presented with the spectral formalism: the emphasis is put on the second-order moments. To this end, the EDQNM approximation is used to close the nonlinear third-order correlations: some generality is kept in the derivations on purpose. Finally, in the framework of IMHDT turbulence, the final equations of the spherically averaged spectra are presented.

2.1. *Spectral evolution equations of magnetohydrodynamics*

The evolution equation of a conducting fluid of fluctuating velocity u_i, submitted to the Laplace force (magnetic part of the Lorentz force), reads

$$\frac{\partial u_i}{\partial t} + u_l \frac{\partial u_i}{\partial x_l} = -\frac{\partial p^*}{\partial x_i} + \nu \frac{\partial^2 u_i}{\partial x_l \partial x_l} + b_l \frac{\partial b_i}{\partial x_l} + B_l^0 \frac{\partial b_i}{\partial x_l}, \qquad (2.1)$$

where b_i is the fluctuating magnetic field, $\boldsymbol{B}^0$ a possible external mean magnetic field, ν the kinematic viscosity and p^* the total pressure. Both u_i and b_i are solenoidal, i.e. $div(\boldsymbol{u}) = div(\boldsymbol{b}) = 0$. The equation of b_i is obtained by combining the Maxwell–Faraday law, the Ohm law (without the Hall term) and the Maxwell–Ampère law, so that

$$\frac{\partial b_i}{\partial t} + u_l \frac{\partial b_i}{\partial x_l} = b_l \frac{\partial u_i}{\partial x_l} + B_l^0 \frac{\partial u_i}{\partial x_l} + \eta \frac{\partial^2 b_i}{\partial x_l \partial x_l}, \qquad (2.2)$$

where η is the magnetic diffusivity, or resistivity. We choose a unit magnetic Prandtl number, so that $\nu = \eta$. When dropping $\boldsymbol{B}^0$ in the latter equation, one remarks that it is similar to the equation of vorticity $\boldsymbol{\omega}$, which is the so-called Batchelor analogy (Batchelor 1950). Furthermore, it is worth noting that $\boldsymbol{b}$ is a pseudo-vector like $\boldsymbol{\omega}$, since it is defined as $\nabla \times \boldsymbol{a}$, where the true vector $\boldsymbol{a}$ is the magnetic potential (some considerations about the modelling of $\boldsymbol{a}$ are proposed in appendix A.1).

The spectral counterpart of (2.1) and (2.2) are given by

$$\left(\frac{\partial}{\partial t} + \nu k^2 \right) \hat{u}_i(\boldsymbol{k}) = -\mathrm{i} P_{imn}(\boldsymbol{k}) \, \widehat{u_m u_n}(\boldsymbol{k}) + \mathrm{i} P_{imn}(\boldsymbol{k}) \, \widehat{b_m b_n}(\boldsymbol{k}) + \mathrm{i} B_l^0 k_l \hat{b}_i(\boldsymbol{k}), \qquad (2.3)$$

$$\left(\frac{\partial}{\partial t} + \eta k^2 \right) \hat{b}_i(\boldsymbol{k}) = -\mathrm{i} k_l \widehat{b_i u_l}(\boldsymbol{k}) + \mathrm{i} k_l \widehat{u_i b_l}(\boldsymbol{k}) + \mathrm{i} B_l^0 k_l \hat{u}_i(\boldsymbol{k}), \qquad (2.4)$$

where the Kraichnan operator is given by $2P_{imn} = k_m P_{in} + k_n P_{im}$, with the projector $P_{ij} = \delta_{ij} - \alpha_i \alpha_j$ and $\alpha_i = k_i/k$, and $\hat{(\cdot)}$ denotes the Fourier transform. In homogeneous

turbulence, the spectral second-order moments of interest, namely the Reynolds tensor $\hat{R}_{ij}$, the magnetic tensor $\hat{B}_{ij}$, and the velocity–magnetic correlation $\hat{H}_{ij}^{c}$, are defined as

$$\hat{R}_{ij}(\boldsymbol{k}, t)\delta(\boldsymbol{k} - \boldsymbol{p}) = \langle \hat{u}_i^*(\boldsymbol{p}, t)\hat{u}_j(\boldsymbol{k}, t)\rangle, \qquad (2.5)$$

$$\hat{B}_{ij}(\boldsymbol{k}, t)\delta(\boldsymbol{k} - \boldsymbol{p}) = \langle \hat{b}_i^*(\boldsymbol{p}, t)\hat{b}_j(\boldsymbol{k}, t)\rangle, \qquad (2.6)$$

$$\hat{H}_{ij}^{c}(\boldsymbol{k}, t)\delta(\boldsymbol{k} - \boldsymbol{p}) = \langle \hat{u}_i^*(\boldsymbol{p}, t)\hat{b}_j(\boldsymbol{k}, t)\rangle, \qquad (2.7)$$

where $(\cdot)^*$ denotes the complex conjugate, and $\langle \cdot \rangle$ an ensemble average. Their evolution equations read

$$\left(\frac{\partial}{\partial t} + 2\nu k^2\right)\hat{R}_{ij}(\boldsymbol{k}) = T_{ij}^{\mathrm{V(hyd)}}(\boldsymbol{k}) + T_{ij}^{\mathrm{V(mag)}}(\boldsymbol{k}) + \mathrm{i}B_l^0 k_l \left(\hat{H}_{ij}^{c}(\boldsymbol{k}) - \hat{H}_{ji}^{c*}(\boldsymbol{k})\right), \qquad (2.8)$$

$$\left(\frac{\partial}{\partial t} + 2\eta k^2\right)\hat{B}_{ij}(\boldsymbol{k}) = T_{ij}^{\mathrm{B(mag)}}(\boldsymbol{k}) + \mathrm{i}B_l^0 k_l \left(\hat{H}_{ji}^{c*}(\boldsymbol{k}) - \hat{H}_{ij}^{c}(\boldsymbol{k})\right), \qquad (2.9)$$

$$\left(\frac{\partial}{\partial t} + (\nu + \eta)k^2\right)\hat{H}_{ij}^{c}(\boldsymbol{k}) = T_{ij}^{c}(\boldsymbol{k}) + \mathrm{i}B_l^0 k_l \left(\hat{R}_{ji}(\boldsymbol{k}) - \hat{B}_{ij}(\boldsymbol{k})\right), \qquad (2.10)$$

where the time dependence has been omitted for clarity. One can note from (2.10) that in the presence of a mean magnetic field $\boldsymbol{B}^0$, kinetic helicity and magnetic helicity could produce the cross-correlation $\hat{H}_{ij}^{c}$. The nonlinear kinetic transfer $T_{ij}^{\mathrm{V(hyd)}}$, which is always present in hydrodynamics turbulence, is the same as in HIT, meaning

$$T_{ij}^{\mathrm{V(hyd)}}(\boldsymbol{k}, t) = P_{imn}(\boldsymbol{k}) \int S_{njm}^{uuu}(\boldsymbol{k}, \boldsymbol{p}, t)\, \mathrm{d}^3\boldsymbol{p} + P_{jmn}(\boldsymbol{k}) \int S_{nim}^{uuu*}(\boldsymbol{k}, \boldsymbol{p}, t)\, \mathrm{d}^3\boldsymbol{p}, \qquad (2.11)$$

where S_{ijn}^{uuu} is the spectral triple velocity correlation

$$S_{ijn}^{uuu}(\boldsymbol{k}, \boldsymbol{p}, t)\delta(\boldsymbol{k} + \boldsymbol{p} + \boldsymbol{q}) = \mathrm{i}\langle \hat{u}_i(\boldsymbol{q}, t)\hat{u}_j(\boldsymbol{k}, t)\hat{u}_n(\boldsymbol{p}, t)\rangle. \qquad (2.12)$$

The nonlinear magnetic transfer $T_{ij}^{\mathrm{V(mag)}}$ represents the retro-action of the magnetic field on the velocity one through the Laplace force, and reads

$$T_{ij}^{\mathrm{V(mag)}}(\boldsymbol{k}, t) = -P_{imn}(\boldsymbol{k}) \int S_{njm}^{ubb}(\boldsymbol{k}, \boldsymbol{p}, t)\, \mathrm{d}^3\boldsymbol{p} - P_{jmn}(\boldsymbol{k}) \int S_{nim}^{ubb*}(\boldsymbol{k}, \boldsymbol{p}, t)\, \mathrm{d}^3\boldsymbol{p}, \qquad (2.13)$$

where S_{ijn}^{ubb} is the spectral velocity–magnetic–magnetic correlation defined as

$$S_{ijn}^{ubb}(\boldsymbol{k}, \boldsymbol{p}, t)\delta(\boldsymbol{k} + \boldsymbol{p} + \boldsymbol{q}) = \mathrm{i}\langle \hat{u}_i(\boldsymbol{q}, t)\hat{b}_j(\boldsymbol{k}, t)\hat{b}_n(\boldsymbol{p}, t)\rangle. \qquad (2.14)$$

Then, for the magnetic equation, one has

$$T_{ij}^{\mathrm{B(mag)}}(\boldsymbol{k}, t) = k_l \int \left(S_{jli}^{ubb*}(\boldsymbol{p}, \boldsymbol{k}, t) + S_{ilj}^{ubb}(\boldsymbol{p}, \boldsymbol{k}, t) - S_{lji}^{ubb*}(\boldsymbol{p}, \boldsymbol{k}, t) - S_{lij}^{ubb}(\boldsymbol{p}, \boldsymbol{k}, t)\right) \mathrm{d}^3\boldsymbol{p}. \qquad (2.15)$$

Finally, for the cross-helicity, the nonlinear transfer involves two additional three-point correlations

$$T_{ij}^{c}(\boldsymbol{k}, t) = k_l \int \left(S_{lji}^{uub*}(\boldsymbol{p}, \boldsymbol{k}, t) - S_{jli}^{uub*}(\boldsymbol{p}, \boldsymbol{k}, t)\right) \mathrm{d}^3\boldsymbol{p}$$

$$+ P_{imn}(\boldsymbol{k}) \int \left(S_{njm}^{uub}(\boldsymbol{k}, \boldsymbol{p}, t) - S_{njm}^{bbb}(\boldsymbol{k}, \boldsymbol{p}, t)\right) \mathrm{d}^3\boldsymbol{p}, \qquad (2.16)$$

with

$$S_{ijn}^{uub}(\boldsymbol{k}, \boldsymbol{p}, t)\delta(\boldsymbol{k}+\boldsymbol{p}+\boldsymbol{q}) = i\langle\hat{u}_i(\boldsymbol{q}, t)\hat{b}_j(\boldsymbol{k}, t)\hat{u}_n(\boldsymbol{p}, t)\rangle, \quad (2.17)$$

$$S_{ijn}^{bbb}(\boldsymbol{k}, \boldsymbol{p}, t)\delta(\boldsymbol{k}+\boldsymbol{p}+\boldsymbol{q}) = i\langle\hat{b}_i(\boldsymbol{q}, t)\hat{b}_j(\boldsymbol{k}, t)\hat{b}_n(\boldsymbol{p}, t)\rangle. \quad (2.18)$$

More details about cross-helical nonlinear transfers are given later in §4 for imbalanced MHD.

2.2. *EDQNM procedure and eddy damping*

In this part, the EDQNM procedure is briefly presented, and more details can be found in Sagaut & Cambon (2008) for the non-conducting case. The first step is to express T_{ijn}^{xxx}, which is the nonlinear transfer in the equation for the triple correlation S_{ijn}^{xxx}, as function of the previous second-order moments thanks to the quasi-normal approximation, where x stands for either u or b. Then, an eddy-damping term is used to model the departure of the statistics from normal laws. In hydrodynamics turbulence, this yields

$$T_{ijn}^{uuu}(\boldsymbol{k}, \boldsymbol{p}) = T_{ijn}^{\mathrm{QN,uuu}}(\boldsymbol{k}, \boldsymbol{p}) - (\mu_1(k) + \mu_1(p) + \mu_1(q))\,S_{ijn}^{uuu}(\boldsymbol{k}, \boldsymbol{p}), \quad (2.19)$$

where $T_{ijn}^{\mathrm{QN,uuu}}$ is the quasi-normal expression of T_{ijn}^{uuu}, and μ_1 is the classical eddy-damping term

$$\mu_1(k, t) = A_1\sqrt{\int_0^k x^2 E_V(x, t)\,\mathrm{d}x}, \quad A_1 = 0.355, \quad (2.20)$$

with E_V the kinetic energy spectrum. This procedure must be repeated in MHD for $T_{ijn}^{\mathrm{QN,bbb}}$, $T_{ijn}^{\mathrm{QN,uub}}$ and $T_{ijn}^{\mathrm{QN,ubb}}$. Using the definitions of the three-point correlations and the expressions of the nonlinear transfers (2.11)–(2.18) one gets after some algebra

$$\begin{aligned}
T_{ijn}^{\mathrm{QN,ubb}}(\boldsymbol{k}, \boldsymbol{p}) = {} & 2P_{jpq}(\boldsymbol{k})\left[\hat{H}_{pi}^c(\boldsymbol{q})\hat{H}_{qn}^c(\boldsymbol{p}) - \hat{B}_{pi}(\boldsymbol{q})\hat{B}_{qn}(\boldsymbol{p})\right] \\
& + p_l\left[\hat{R}_{lj}(\boldsymbol{k})B_{ni}(\boldsymbol{q}) + \hat{H}_{li}^c(\boldsymbol{q})\hat{H}_{jn}^c(-\boldsymbol{k}) - \hat{H}_{ni}^c(\boldsymbol{q})\hat{H}_{jl}^c(-\boldsymbol{k}) - \hat{R}_{nj}(\boldsymbol{k})B_{li}(\boldsymbol{q})\right] \\
& + q_l\left[\hat{R}_{lj}(\boldsymbol{k})B_{in}(\boldsymbol{p}) + \hat{H}_{ln}^c(\boldsymbol{p})\hat{H}_{ji}^c(-\boldsymbol{k}) - \hat{H}_{in}^c(\boldsymbol{p})\hat{H}_{jl}^c(-\boldsymbol{k}) - \hat{R}_{ij}(\boldsymbol{k})B_{ln}(\boldsymbol{p})\right],
\end{aligned}$$

$$(2.21)$$

$$\begin{aligned}
T_{ijn}^{\mathrm{QN,uub}}(\boldsymbol{k}, \boldsymbol{p}) = {} & 2P_{npq}(\boldsymbol{p})\left[\hat{H}_{pj}^c(\boldsymbol{k})\hat{R}_{qi}(\boldsymbol{q}) - \hat{B}_{pj}(\boldsymbol{k})\hat{H}_{iq}^c(-\boldsymbol{q})\right] \\
& + 2P_{ipq}(\boldsymbol{q})\left[\hat{H}_{pj}^c(\boldsymbol{k})\hat{R}_{qn}(\boldsymbol{p}) - \hat{B}_{pj}(\boldsymbol{k})\hat{H}_{nq}^c(-\boldsymbol{p})\right] \\
& + k_l\left[\hat{H}_{ij}^c(-\boldsymbol{q})\hat{R}_{ln}(\boldsymbol{p}) + \hat{H}_{nj}^c(-\boldsymbol{p})\hat{R}_{li}(\boldsymbol{q}) - \hat{H}_{nl}^c(-\boldsymbol{p})\hat{R}_{ji}(\boldsymbol{q}) - \hat{H}_{il}^c(-\boldsymbol{q})\hat{R}_{jn}(\boldsymbol{p})\right],
\end{aligned}$$

$$(2.22)$$

$$\begin{aligned}
T_{ijn}^{\mathrm{QN,bbb}}(\boldsymbol{k}, \boldsymbol{p}) = {} & k_l\left[\hat{H}_{li}^c(\boldsymbol{q})\hat{B}_{jn}(\boldsymbol{p}) + \hat{H}_{ln}^c(\boldsymbol{p})\hat{B}_{ji}(\boldsymbol{q}) - \hat{H}_{ji}^c(\boldsymbol{q})\hat{B}_{ln}(\boldsymbol{p}) - \hat{H}_{jn}^c(\boldsymbol{p})\hat{B}_{li}(\boldsymbol{q})\right] \\
& + p_l\left[\hat{H}_{li}^c(\boldsymbol{q})\hat{B}_{nj}(\boldsymbol{k}) + \hat{B}_{ni}(\boldsymbol{q})\hat{H}_{lj}^c(\boldsymbol{k}) - \hat{H}_{ni}^c(\boldsymbol{q})\hat{B}_{lj}(\boldsymbol{k}) - \hat{H}_{nj}^c(\boldsymbol{k})\hat{B}_{li}(\boldsymbol{q})\right] \\
& + q_l\left[\hat{H}_{ln}^c(\boldsymbol{p})\hat{B}_{ij}(\boldsymbol{k}) + \hat{B}_{in}(\boldsymbol{p})\hat{H}_{lj}^c(\boldsymbol{k}) - \hat{H}_{in}^c(\boldsymbol{p})\hat{B}_{lj}(\boldsymbol{k}) - \hat{H}_{ij}^c(\boldsymbol{k})\hat{B}_{ln}(\boldsymbol{p})\right].
\end{aligned}$$

$$(2.23)$$

These expressions are the most general one can get: only homogeneity was assumed, not isotropy. They could be simplified by using classical $p \leftrightarrow q$ symmetry. Hereafter, isotropic MHD turbulence is considered, so that there is no mean magnetic field $\boldsymbol{B}^0$. Firstly, in this framework with mirror symmetry invariance, also called isotropic balanced MHD, the cross-correlation $\hat{H}_{ij}^c$ vanishes so that $\mathcal{T}_{imn}^{\mathrm{QN,uub}} = \mathcal{T}_{imn}^{\mathrm{QN,bbb}} = 0$, and only part of $\mathcal{T}_{imn}^{\mathrm{QN,ubb}}$ remains. The kinetic and magnetic helicities, contained in $\hat{R}_{ij}$ and $\hat{B}_{ij}$ and defined in the following section for generality purposes, are zero as well. Non-zero cross-helicity is considered in §4.

Moreover, as intensively discussed in Pouquet *et al.* (1976), Baerenzung *et al.* (2008), an additional eddy-damping term μ_A should be added to μ_1 to take into account the propagation of Alfvén waves, where

$$\mu_A(k, t) = \sqrt{\frac{2}{3}} \, k \sqrt{\int_0^k E_B(x, t)\, \mathrm{d}x}, \qquad (2.24)$$

where E_B is the magnetic energy spectrum. Furthermore E_V is replaced in (2.20) by the total energy spectrum $E = E_V + E_B$, linked to the inviscid invariant total energy. The constant in μ_A is chosen so that when $k \to \infty$, μ_A is the Alfvén time: $\mu_A^{-1} = (kb_0)^{-1} = \tau_A$, where the magnetic energy in IMHDT reads $3b_0^2/2$.

Combining the quasi-normal approximation, the eddy-damping terms and the classical Markovianization step to ensure realizability of the spectra in HIT (Orszag 1970; Lesieur 2008; Sagaut & Cambon 2008), it is possible to express the triple correlations as function of the second-order moments for MHD, thus permitting to close the evolution equations (2.8)–(2.10)

$$S_{ijn}^{\mathrm{xxx}}(\boldsymbol{k}, \boldsymbol{p}, t) = \theta_{kpq} \mathcal{T}_{ijn}^{\mathrm{QN,xxx}}(\boldsymbol{k}, \boldsymbol{p}, t), \qquad (2.25)$$

where θ_{kpq} is the characteristic time of the third-order correlations, containing the eddy-damping terms, according to

$$\theta_{kpq} = \frac{1 - \mathrm{e}^{-\mu_{kpq}t}}{\mu_{kpq}}, \quad \mu_{kpq} = \mu_k + \mu_p + \mu_q, \quad \mu_k = (\nu + \eta)k^2 + \mu_1(k) + \mu_A(k).$$
$$(2.26a\text{-}c)$$

One can observe in figure 1(*a*) that $\mu_A > \mu_1$ in the entire inertial range, so that μ_A^{-1} becomes the smallest time scale of the problem. The inertial scaling of the total energy spectrum being determined by the smallest time scale through nonlinear transfers (Lee *et al.* 2010), it follows that the choice of μ_A prescribes the inertial scaling of the total energy spectrum E: within this isotropic EDQNM modelling, this amounts to $E \sim k^{-3/2}$ as revealed in §3. This is also true in the presence of cross-helicity, see later in §4. Note that if one does not ensure $\mu_A > \mu_1$, realizability is not guaranteed anymore, meaning that either E_V or E_B can become negative. Consequently in what follows, we do not investigate whether one has $E \sim k^{-3/2}$ or $E \sim k^{-5/3}$ in IMHDT, but rather the asymptotic results one can obtain from a given inertial scaling.

Moreover, it appears in figure 1(*a*) that for sufficiently large k, one has $\mu_A(k) \sim k$, as expected (Pouquet *et al.* 1976). Indeed, as previously mentioned, when $k \to \infty$, one has $\mu_A \simeq kb_0$ since $\int_0^\infty E_B \, \mathrm{d}k = 3b_0^2/2$. This further illustrates that the Alfvén time $\tau_A = (kb_0)^{-1}$ is the characteristic time of the inertial range. Also, in the inertial range, the classical eddy-damping part μ_1 evolves as $k^{3/4}$, which is consistent with previous arguments: from its definition (2.20), dimensional analysis yields $\mu_1 \sim \sqrt{k^3 E} = (\epsilon b_0 k^3)^{1/4}$: this is different from HIT where $\mu_1 \sim \tau_V^{-1} \sim (k^2 \epsilon_V)^{1/3}$.
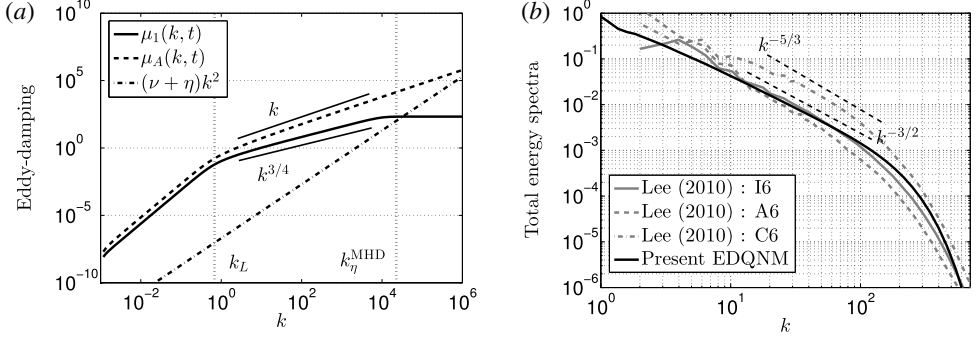
FIGURE 1. (*a*) Different contributions in the eddy-damping term μ_k, defined in (2.26), of the characteristic time θ_{kpq} at $Re_\lambda = 6 \times 10^3$, along with the integral and dissipative wavenumbers k_L and k_η^{MHD}, defined later on. (*b*) Total energy spectrum $E(k, t)$, with initial condition (2.44) and $E_V(k, t = 0) = 0$ at $Re_\lambda = 260$, compared to spectra obtained in Lee *et al.* (2010) with various initial conditions (I6, A6, C6).

2.3. *Spherically averaged equations for isotropic MHD*

In isotropic MHD turbulence without a mean magnetic field, the solenoidal spectral tensors $\hat{R}_{ij}$ and $\hat{B}_{ij}$ are decomposed as

$$\hat{R}_{ij}(\boldsymbol{k}, t) = P_{ij}(\boldsymbol{k})\mathcal{E}^V(\boldsymbol{k}, t) + \text{i}\epsilon_{ijn}\alpha_n\frac{\mathcal{H}^V(\boldsymbol{k}, t)}{k}, \tag{2.27}$$

$$\hat{B}_{ij}(\boldsymbol{k}, t) = P_{ij}(\boldsymbol{k})\mathcal{E}^B(\boldsymbol{k}, t) + \text{i}\epsilon_{ijn}\alpha_n\frac{\mathcal{H}^B(\boldsymbol{k}, t)}{k}, \tag{2.28}$$

where $\mathcal{E}^V$ and $\mathcal{E}^B$ are the kinetic and magnetic energy densities, and $\mathcal{H}^V$ and $\mathcal{H}^B$ are the kinetic and 'super' magnetic helicity densities, given by

$$\mathcal{E}^V(\boldsymbol{k}, t) = \tfrac{1}{2}\hat{R}_{ii}(\boldsymbol{k}, t), \quad \mathcal{H}^V(\boldsymbol{k}, t) = -\tfrac{1}{2}\text{i}\epsilon_{ijl}k_l\hat{R}_{ij}(\boldsymbol{k}, t). \tag{2.29a,b}$$

The definitions are similar for $\mathcal{E}^B$ and $\mathcal{H}^B$. At this point, it is of importance to precise that the magnetic helicity H_M, which is an inviscid invariant of the MHD equations, is linked to $\mathcal{H}^B$ through

$$H_M(t) = \frac{1}{2}\langle \boldsymbol{a} \cdot \boldsymbol{b} \rangle = \int k^{-2}\mathcal{H}^B(\boldsymbol{k}, t)\,\text{d}^3\boldsymbol{k}, \quad \frac{1}{2}\langle \boldsymbol{j} \cdot \boldsymbol{b} \rangle = \int \mathcal{H}^B(\boldsymbol{k}, t)\,\text{d}^3\boldsymbol{k}, \tag{2.30a,b}$$

with $\boldsymbol{j}$ the normalized current density. In the following developments, IMHDT is considered (with mirror symmetry) so that both $\mathcal{H}^V$ and $\mathcal{H}^B$ vanish. Then, the evolution equations of the energy densities $\mathcal{E}^V$ and $\mathcal{E}^B$ read

$$\left(\frac{\partial}{\partial t} + 2\nu k^2\right)\mathcal{E}^V(\boldsymbol{k}, t) = T_\mathcal{E}^{\text{V(hyd)}}(\boldsymbol{k}, t) + T_\mathcal{E}^{\text{V (mag)}}(\boldsymbol{k}, t), \tag{2.31}$$

$$\left(\frac{\partial}{\partial t} + 2\eta k^2\right)\mathcal{E}^B(\boldsymbol{k}, t) = T_\mathcal{E}^{\text{B(mag)}}(\boldsymbol{k}, t), \tag{2.32}$$

where the nonlinear transfers are given by

$$T_\mathcal{E}^{\text{V(hyd)}}(\boldsymbol{k}, t) = \frac{1}{2}T_{ii}^{\text{V(hyd)}}(\boldsymbol{k}, t) = P_{imn}(\boldsymbol{k})\int \Re\left(S_{nim}^{uuu}(\boldsymbol{k}, \boldsymbol{p}, t)\right)\text{d}^3\boldsymbol{p}, \tag{2.33}$$

$$T_{\mathcal{E}}^{\text{V(mag)}}(\boldsymbol{k}, t) = \frac{1}{2} T_{ii}^{\text{V(mag)}}(\boldsymbol{k}, t) = -P_{imn}(\boldsymbol{k}) \int \Re\left(S_{nim}^{ubb}(\boldsymbol{k}, \boldsymbol{p}, t)\right) \mathrm{d}^3\boldsymbol{p}, \qquad (2.34)$$

$$T_{\mathcal{E}}^{\text{B(mag)}}(\boldsymbol{k}, t) = \frac{1}{2} T_{ii}^{\text{B(mag)}}(\boldsymbol{k}, t) = k_l \int \Re\left(S_{ili}^{ubb}(\boldsymbol{p}, \boldsymbol{k}, t) - S_{lii}^{ubb}(\boldsymbol{p}, \boldsymbol{k}, t)\right) \mathrm{d}^3\boldsymbol{p}, \quad (2.35)$$

with $\Re$ denoting the real part. The final equations for isotropic MHD turbulence are obtained by spherically averaging the evolution equations (2.31)–(2.32) of $\mathcal{E}^V$ and $\mathcal{E}^B$: the kinetic energy and magnetic energy spectra are then defined as

$$E_V(k, t) = \int_{S_k} \mathcal{E}^V(\boldsymbol{k}, t) \, \mathrm{d}^2\boldsymbol{k}, \quad E_B(k, t) = \int_{S_k} \mathcal{E}^B(\boldsymbol{k}, t) \, \mathrm{d}^2\boldsymbol{k}, \qquad (2.36a,b)$$

where S_k is a sphere of radius k. From the definitions of the kinetic and magnetic spectra and equations (2.31)–(2.32), one straightforwardly obtains

$$\left(\frac{\partial}{\partial t} + 2\nu k^2\right) E_V(k, t) = S^{\text{V(hyd)}}(k, t) + S^{\text{V(mag)}}(k, t) = S^{\text{V}}(k, t), \qquad (2.37)$$

$$\left(\frac{\partial}{\partial t} + 2\eta k^2\right) E_B(k, t) = S^{\text{B(mag)}}(k, t). \qquad (2.38)$$

The spherically averaged nonlinear kinetic hydrodynamic transfer is

$$\begin{aligned}
S^{\text{V(hyd)}}(k, t) &= \int_{S_k} T_{\mathcal{E}}^{\text{V(hyd)}}(\boldsymbol{k}, t) \, \mathrm{d}^2\boldsymbol{k} \\
&= 16\pi^2 \int_{\Delta_k} \theta_{kpq} k^2 p^2 q(xy + z^3) \mathcal{E}_0^{V''}(\mathcal{E}_0^{V'} - \mathcal{E}_0^V) \, \mathrm{d}p \, \mathrm{d}q, \qquad (2.39)
\end{aligned}$$

with Δ_k the domain where k, p and q are the lengths of the sides of the triangle formed by the triad, and x, y and z are the cosines of the angles formed by $\boldsymbol{p}$ and $\boldsymbol{q}$, $\boldsymbol{q}$ and $\boldsymbol{k}$ and $\boldsymbol{k}$ and $\boldsymbol{p}$. The spherically averaged nonlinear kinetic MHD transfer reads

$$\begin{aligned}
S^{\text{V(mag)}}(k, t) &= \int_{S_k} T_{\mathcal{E}}^{\text{V(mag)}}(\boldsymbol{k}, t) \, \mathrm{d}^2\boldsymbol{k} \\
&= 16\pi^2 \int_{\Delta_k} \theta_{kpq} k^2 p^2 qz(1 - y^2) \mathcal{E}_0^{B''}(\mathcal{E}_0^{B'} - \mathcal{E}_0^V) \, \mathrm{d}p \, \mathrm{d}q, \qquad (2.40)
\end{aligned}$$

and the spherically averaged nonlinear magnetic transfer is

$$\begin{aligned}
S^{\text{B(mag)}}(k, t) &= \int_{S_k} T_{\mathcal{E}}^{\text{B(mag)}}(\boldsymbol{k}, t) \, \mathrm{d}^2\boldsymbol{k} \\
&= 16\pi^2 \int_{\Delta_k} \theta_{kpq} k^2 p^2 q \left((xy + z)\mathcal{E}_0^{V''}(\mathcal{E}_0^{B'} - \mathcal{E}_0^B) + z(1 - x^2)\mathcal{E}_0^{B''}(\mathcal{E}_0^{V'} - \mathcal{E}_0^B)\right) \mathrm{d}p \, \mathrm{d}q,
\end{aligned}$$
$$(2.41)$$

where $\mathcal{E}_0^V = E_V(k)/(4\pi k^2)$, $\mathcal{E}_0^{V'} = E_V(p)/(4\pi p^2)$, $\mathcal{E}_0^{V''} = E_V(q)/(4\pi q^2)$ and similarly for the magnetic energy spectrum. About the nonlinear transfers: $S^{\text{V(hyd)}}$ is conservative, with zero integral over k, whereas only the sum $S^{\text{V(mag)}} + S^{\text{B(mag)}}$ is conservative. The expressions of the two later transfer terms are in agreement with Kraichnan & Nagarajan (1967), Zhou, Schilling & Ghosh (2002), and there are typo errors in

Pouquet *et al.* (1976), Müller & Grappin (2004), Baerenzung *et al.* (2008). The typos in the reference paper Pouquet *et al.* (1976) were corrected in Léorat, Pouquet & Frisch (1981), precisely pages 441–442 therein.

The kinetic energy and its dissipation rate are given by

$$K_V = \frac{1}{2}\langle u_i u_i \rangle = \int_0^\infty E_V(k)\,\mathrm{d}k, \quad \epsilon_V = \nu \left\langle \frac{\partial u_i}{\partial x_j}\frac{\partial u_i}{\partial x_j} \right\rangle = 2\nu \int_0^\infty k^2 E_V(k)\,\mathrm{d}k. \quad (2.42a,b)$$

The magnetic quantities are obtained by changing $()_V \to ()_B$, $u_i \to b_i$ and $\nu \to \eta$. Since only the total energy $K = K_V + K_B$ is an inviscid invariant of MHD, we define also the total energy dissipation rate as $\epsilon = \epsilon_V + \epsilon_B$, and the integral scale as

$$L = \frac{3\pi}{4K} \int_0^\infty \frac{E_V(k) + E_B(k)}{k}\,\mathrm{d}k. \quad (2.43)$$

Further information about the evolution equations of the total energy K and total dissipation ϵ can be found in appendix B.1.

2.4. *Numerical set-up and initial conditions*

The time evolution of the kinetic and magnetic spectra $E_V(k,t)$ and $E_B(k,t)$ is obtained by solving two coupled integro-differential equations using a third-order Runge–Kutta scheme with implicit treatment of viscous terms. The wavenumber space is discretized using a logarithmic mesh $k_{i+1} = r k_i$ for $i = 1, \ldots, n$, where n is the total number of modes and $r = 10^{1/f}$, $f = 15$ is the number of points per decade. This mesh spans from $k_{\min} = 10^{-4} k_L$ to $k_{\max} = 10 k_\eta$, where $k_L = 1/L$ is the integral wavenumber, and $k_\eta = (\epsilon/\nu^3)^{1/4}$ is the Kolmogorov wavenumber. It will be shown hereafter that the relevant dissipation wavenumber k_η^{MHD} for MHD is smaller than k_η. The characteristic time used for normalization is the eddy turnover time $\tau_0 = K(0)/\epsilon(0)$. The initial Reynolds number is varied between $5 \times 10^3 \leqslant Re_\lambda(0) \leqslant 5 \times 10^4$ depending on the cases considered.

The following initial condition is chosen for the magnetic energy spectrum if not mentioned otherwise

$$E_B(k, t=0) = C_B k^{\sigma_B} \exp\left(-\frac{\sigma_B}{2}k^2\right), \quad (2.44)$$

with C_B so that $\int_0^\infty E_B(k,\ t=0)\,\mathrm{d}k = 1$. The kinetic energy spectrum is initially either zero, or equal to E_B: the following results, and notably the inertial scalings and decay laws, are not modified asymptotically by choosing different initial relative intensities between the kinetic and magnetic fields. In both cases, the infrared slope σ_B of the magnetic energy spectrum is the large scale initial condition (recall that in hydrodynamics turbulence, the infrared slopes $\sigma_V = 2$ and $\sigma_V = 4$ for the kinetic energy spectrum correspond respectively to Saffman and Batchelor turbulence). In agreement with classical arguments given in Lesieur & Ossia (2000), Lesieur (2008), if initially zero, E_V has an infrared slope $\sigma_V = 4$ once created. If $E_V = E_B$ initially, then $\sigma_V = \sigma_B$. A particular attention has to be given to the time step. Indeed in MHD, one needs to take into account the characteristic propagation time of Alfvén waves $\tau_A \sim (kb_0)^{-1}$. This is essential and considerably reduces the time step. Consequently, even with EDQNM, the duration of the simulations can be rather long at large Reynolds numbers if one wants to capture several turnover times, but is still much less than with DNS.

3. The decay of balanced isotropic MHD turbulence

In the following parts, balanced IMHDT is considered, meaning that the cross-helicity is zero: $\langle \boldsymbol{u} \cdot \boldsymbol{b} \rangle = 0$. The imbalanced case is addressed in §4. First, spectral scalings for the kinetic, magnetic and total energy spectra $E_V(k, t)$, $E_B(k, t)$ and $E(k, t)$, are presented within the EDQNM modelling, and compared to spectra obtained in Lee *et al.* (2010). The different characteristic time scales involved in the dynamics and the nonlinear transfers are studied as well. Finally, the decay of the total energy of the flow is analysed: theoretical predictions are derived and assessed numerically, which is the most important contribution of this work for balanced MHD. Note that the scaling of the residual energy spectrum is addressed in appendix A.2.

3.1. *Kinetic energy and magnetic spectra $E_V(k, t)$ and $E_B(k, t)$*

The phenomenological arguments given by Kraichnan (1965) to derive the $k^{-3/2}$ isotropic inertial scaling are first briefly recalled. Unlike HIT where the local time of the cascade is $\tau_V = (k^3 E_V)^{-1/2}$, the characteristic transfer time τ_{tr} of energy in MHD is longer. This MHD transfer time τ_{tr} can be seen as the characteristic time of waves packet distortion, and is linked to the characteristic Alfvén time $\tau_A \sim (kb_0)^{-1}$ which reflects the duration of interactions between two counter-propagating Alfvén waves. Indeed, in Kraichnan's phenomenology, the transfer of energy at a scale $l \sim k^{-1}$ results from the cumulative effects of multiple interactions and collisions between counter propagating Alfvén wave packets, which evolve along the magnetic field of scales larger than *l*. Consequently, the transfer time in MHD turbulence is $\tau_{\mathrm{tr}} = \tau_V^2/\tau_A \sim lb_0/u^2$ (Pouquet 1996; Gomez, Politano & Pouquet 1999; Galtier 2016), unlike HIT where $\tau_{\mathrm{tr}} = \tau_V \sim l/u$. From these considerations, one can express the total energy dissipation rate ϵ as the ratio of the local square velocity $u^2 \sim (kE)$ to the transfer time according to

$$\epsilon \sim \frac{kE(k)}{\tau_{\mathrm{tr}}} \sim \frac{kE(k)\tau_A}{\tau_V^2} \sim \frac{kE(k)(kb_0)^{-1}}{(k^3 E)^{-1}} = k^3 b_0^{-1} E(k)^2, \tag{3.1}$$

so that one has in the inertial range

$$E(k, t) = C_{\mathrm{IK}}\sqrt{\epsilon b_0}\, k^{-3/2}. \tag{3.2}$$

This scaling is referred to as the Iroshnikov–Kraichnan (IK) one, and this analysis also gives that E_V and E_B have a $k^{-3/2}$ inertial scaling like E. The constant is found here to be of order $2 \leqslant C_{\mathrm{IK}} \leqslant 3$ for $10^3 \leqslant Re_\lambda \sim 10^4$, which is higher than the Kolmogorov constant in HIT, and this feature is in agreement with Beresnyak (2011).

Within the isotropic EDQNM framework, the $k^{-3/2}$ scaling is a consequence of the choice of the additional eddy-damping term μ_A defined in (2.24). This is illustrated in figure 2 for $\sigma_B = 2$. Note that the $k^{-3/2}$ inertial scaling also holds for E_+ and E_- associated with the Elsässer variables $z^\pm = \boldsymbol{u} \pm \boldsymbol{b}$. The kinetic energy spectrum, initially zero in figure 2, is created within the first turnover time by $S^{\mathrm{V(mag)}}$, with an infrared slope $\sigma_V = 4$, and consequently experiences a backscatter of energy (Lesieur & Ossia 2000). Whereas at large scales the magnetic spectrum scales with $E_B \sim k^2$. Two other cases ($\sigma_B = 4$ with $E_V = 0$; $\sigma_B = 2$ with $E_V = E_B$) presented in appendix A.2 show that the $k^{-3/2}$ inertial scaling is independent of initial conditions after a few turnover times. This notably implies that the inertial scaling does not depend on the kinetic to magnetic energy ratio K_V/K_B, which only slightly varies with initial conditions (see later figure 11(*d*)).
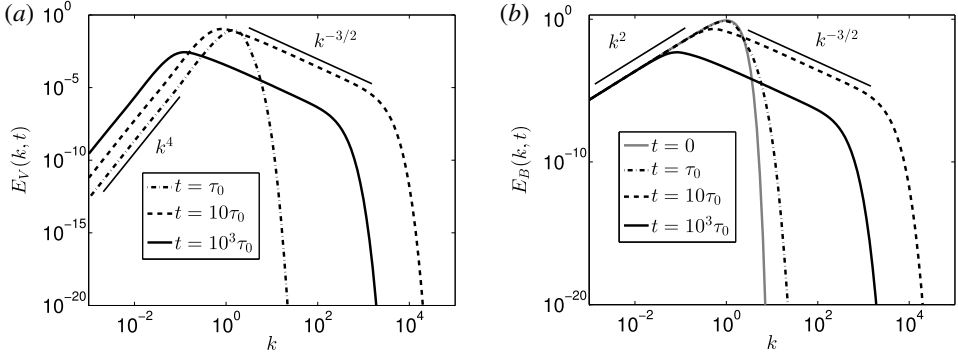
FIGURE 2. Time evolution of the kinetic energy and magnetic energy spectra $E_V(k, t)$ and $E_B(k, t)$ for $\sigma_B = 2$, from $t = 0$ to $t = 10^3\tau_0$, with initially $E_V = 0$. (*a*) Kinetic energy spectrum $E_V(k, t)$. (*b*) Magnetic energy spectrum $E_B(k, t)$.

This $k^{-3/2}$ scaling for E_V and E_B is in agreement with numerical simulations of IMHDT (Grappin *et al.* 1982; Mininni & Pouquet 2007; Yoshimatsu 2012). However, still in the isotropic case, some studies report rather a Kolmogorov $k^{-5/3}$ inertial scaling, at odds with the previous IK $k^{-3/2}$ inertial scaling (Müller & Biskamp 2000; Müller & Grappin 2004, 2005; Alexakis, Mininni & Pouquet 2005). Finally, in some cases both scalings are possible (Haugen, Brandenburg & Dobler 2004; Lee *et al.* 2010; Alexakis 2013), depending on the Reynolds number, the possible forcing terms and initial parameters. The total energy spectrum $E(k, t)$, obtained with EDQNM and the initial condition (2.44) with $E_V(k, t = 0) = 0$, is presented in figure 1(*b*) at moderate Reynolds numbers, and compared to spectra obtained by Lee *et al.* (2010) for different initial conditions. One can see that at $Re_\lambda = 260$, the difference between the $k^{-5/3}$ and $k^{-3/2}$ inertial scalings is quite subtle. Above all, our spectrum E is consistently contained between the different DNS results, obtained after six turnover times, thus showing some quantitative good agreement between EDQNM and DNS.

3.2. *Spectral kinetic and magnetic nonlinear transfers*

The emphasis is now put on the nonlinear transfers of kinetic and magnetic energies. It is firstly observed in figure 3(*a*) that all kinetic and magnetic spherically averaged nonlinear transfer terms bring energy from large to small scales, in agreement with Alexakis *et al.* (2005). The fluxes, computed according to $\Pi(k) = -\int_0^k S(p)\,\mathrm{d}p$, reveal several important features:

(i) The purely hydrodynamic isotropic kinetic flux $\Pi^{V(hyd)}$ is conservative.
(ii) The magnetic part $\Pi^{V(mag)}$ of the total kinetic flux $\Pi^V = \Pi^{V(hyd)} + \Pi^{V(mag)}$ is not conservative, so that Π^V is not.
(iii) The total magnetic flux $\Pi^{(mag)} = \Pi^{B(mag)} + \Pi^{V(mag)}$ is conservative, in agreement with pioneering developments in Kraichnan & Nagarajan (1967).
(iv) Finally, consistently with the total energy being an inviscid invariant, the total flux $\Pi^{V(tot)} = \Pi^{V(hyd)} + \Pi^{V(mag)} + \Pi^{B(mag)}$ is conservative.

One can remark in figure 3(*a*) that the dissipative wavenumber displayed is not the Kolmogorov wavenumber $k_\eta = (\epsilon_V/\nu^3)^{1/4}$, but its equivalent for MHD turbulence, namely k_η^{MHD} (Biskamp & Welter 1989; Diamond & Biskamp 1990; Pouquet 1996).
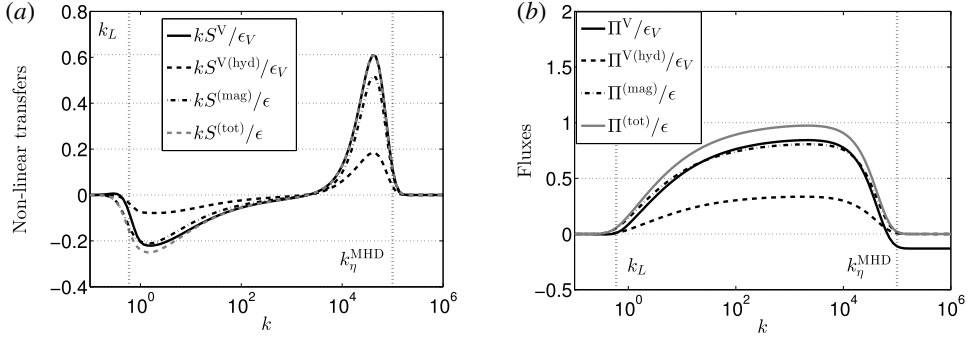
FIGURE 3. Kinetic and magnetic normalized nonlinear transfers and fluxes, at $Re_\lambda \simeq 10^4$, for $\sigma_B = 2$, along with the integral and dissipative wavenumbers k_L, and k_η^{MHD}. (a) Kinetic $S^{\text{V(hyd)}} + S^{\text{V(mag)}} = S^{\text{V}}$ and magnetic $S^{\text{(mag)}} = S^{\text{V(mag)}} + S^{\text{B(mag)}}$ nonlinear transfers. (b) Corresponding kinetic and magnetic fluxes.

This characteristic wavenumber is obtained by equating $(\nu k_\eta^{\text{MHD}2})^{-1}$ and $\tau_{\text{tr}}(k_\eta^{\text{MHD}}) = \sqrt{b_0/\epsilon k_\eta^{\text{MHD}}}$, so that

$$k_\eta^{\text{MHD}} = \left(\frac{\epsilon}{b_0 \nu^2}\right)^{1/3}. \tag{3.3}$$

The fact that k_η^{MHD} is more relevant than k_η in MHD turbulence is illustrated in figure 11 in appendix A.2.

3.3. *Decay of the total energy $K(t)$*

In this part, the decay of the total energy $K = K_V + K_B$ in isotropic MHD turbulence, which evolves according to $\mathrm{d}K/\mathrm{d}t = -\epsilon$ is addressed. One can define the algebraic time exponents α and α_L as $K \sim t^\alpha$ and $L \sim t^{\alpha_L}$, where L is the total integral scale, defined in (2.43). It is assumed for the developments hereafter that the kinetic and magnetic integral scales evolve similarly, which is assessed numerically. From figure 2 and the IK scaling (3.2), it was shown that in the inertial range, the total energy spectrum scales in $E = E_V + E_B \sim \sqrt{\epsilon b_0} k^{-3/2}$. Secondly, at large scales, the infrared slope of E is the one of the most energetic (smallest infrared slope) spectrum: given the initial conditions (2.44) chosen here, one has $E \sim k^{\sigma - p}$, with $\sigma = \sigma_B$, and where p is a backscatter parameter which accounts for strong inverse transfers in hydrodynamics Batchelor turbulence (Lesieur & Ossia 2000; Meldi & Sagaut 2013a; Briard *et al.* 2015).

The prediction of the decay of the total energy in MHD turbulence was addressed in several papers (Hossain *et al.* 1995; Pouquet 1996; Galtier *et al.* 1997, 1999; Kalelkar & Pandit 2004; Banerjee & Jedamzik 2004). Since in Hossain *et al.* (1995) the infrared slopes of the spectra are not considered, we rather focus on the other references. Notably, in Galtier *et al.* (1997), the predictions are, for the total energy and the integral scale,

$$\alpha = -\frac{\sigma + 1}{\sigma + 2}, \quad \alpha_L = \frac{1}{\sigma + 2}. \tag{3.4a,b}$$

These predictions were assessed in two-dimensional simulations in Galtier *et al.* (1997) within the first 10 turnover times, and are further analysed in Galtier *et al.* (1999). One

of the conclusions of these theoretical decay exponents is that MHD turbulence decays more slowly than non-magnetic isotropic turbulence. This is nevertheless at odds with Banerjee & Jedamzik (2004), where stronger decay rates for the kinetic and magnetic energies are obtained, closer to HIT predictions than (3.4).

However, two-dimensional turbulence might be more representative of strong MHD turbulence, where the cascade of energy occurs preferentially in the direction perpendicular to the mean magnetic field $\boldsymbol{B}^0$, than isotropic MHD turbulence with no mean magnetic field. In this view, we propose new theoretical time exponents for the total energy and the integral scale in IMHDT. The method is similar to what is done in HIT (George 1992), and extended to MHD in Pouquet (1996), Galtier *et al.* (1997).

First, for a total energy spectrum scaling in $E \sim k^{\sigma - p}$ at large scales, the total energy evolves as $K \sim L^{-(\sigma - p + 1)} \sim t^{-\alpha_L(\sigma - p + 1)}$, with $L \sim t^{\alpha_L}$. Since $K \sim t^{\alpha}$, one gets

$$\alpha = -(\sigma - p + 1)\alpha_L. \tag{3.5}$$

This relation, also verified in HIT, is given in Galtier *et al.* (1997) without the backscatter parameter p. The second step is to link the decay exponent $\alpha - 1$ of the total dissipation rate ϵ to the expression (3.5). In HIT, one uses $\epsilon_V \sim u^3/L_V$ (George 1992). For MHD turbulence, (3.1) is used instead, with $\tau_{tr} = Lb_0/u^2$, so that $\epsilon \sim u^4/(Lb_0)$. From this point, our development differs from Galtier *et al.* (1997): in the latter reference, $b_0 \sim B_0$ is independent of time and might reflect a background mean magnetic field. This gives $\alpha = \alpha_L - 1$ so that (3.4) is recovered.

On the contrary, we claim that in isotropic MHD turbulence without mean magnetic field, $b_0 = \sqrt{2K_B/3}$ varies with time because the magnetic energies does. Furthermore, we assume that total, kinetic and magnetic energies, have the same asymptotic decay exponent α, even if they have different intensities, so that $b_0 \sim t^{\alpha/2}$. This provides $\alpha_L = 1 + \alpha/2$. Combined with (3.5), this eventually yields our theoretical predictions for the decay of the total energy and integral scale in isotropic MHD turbulence

$$\alpha_L = \frac{2}{\sigma - p + 3}, \quad \alpha = -2\frac{\sigma - p + 1}{\sigma - p + 3}, \quad \begin{cases} p(\sigma = 4) = 1/3, \\ p(\sigma \leqslant 3) = 0. \end{cases} \tag{3.6a-c}$$

The striking feature is that these predictions are identical to the predictions for kinetic energy in HIT (Meldi & Sagaut 2013*a*; Briard *et al.* 2015), despite the non-Kolmogorov scaling of both $E_V(k, t)$ and $E_B(k, t)$. Only the backscatter parameter p is changed for $\sigma = 4$ from $p = 0.55$ in HIT to $p = 1/3$ in IMHDT, which is a rather small difference. These theoretical decay rates span from -1 for $\sigma = 1$ to -1.4 for $\sigma = 4$: these values are closer to the three-dimensional simulations of Banerjee & Jedamzik (2004) than the two-dimensional ones of Galtier *et al.* (1997). Note that our prediction (3.6) is in agreement with the self-similar analysis of Campanelli (2016).

These new predictions for K and L are successfully assessed numerically in figure 4 for $\sigma_B = 2$ and $\sigma_B = 4$. Supplementary simulations revealed that both the decay exponents of kinetic energy α_V and magnetic energy α_B are in agreement with (3.6) for the different initial conditions investigated in appendix A.2: in particular, if $\sigma_B = \sigma = 2$ and $\sigma_V = 4$, one has still $\alpha_V = \alpha_B = \alpha$ since the large scale dynamics is driven by the magnetic field. Also, even though not presented here, we obtained that (i) the decay exponent α of the total energy follows the usual predictions for kinetic energy in HIT at low Reynolds numbers as well; (ii) in the saturated case where $k_{min}/k_L(0) = 1$, one has $K \sim t^{-2}$, like kinetic energy in HIT (take $\sigma \to \infty$ in (3.6));
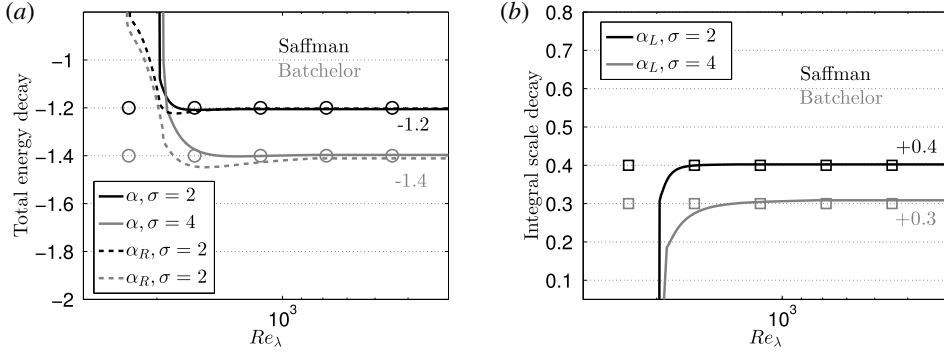
FIGURE 4. Time exponents α and α_L of the total energy K and integral scale L for $\sigma = 2$ (black) and $\sigma = 4$ (grey), with initial conditions (2.44). Lines represent the present simulations, and symbols the theoretical predictions (3.6); $\bigcirc$ for α and $\square$ for α_L. (*a*) Total energy (——); see appendix A.2 for the decay exponent α_R of residual energy (−−). (*b*) Integral scale growth.

and (iii) the value of α, for a given σ, is independent of the kinetic to magnetic energy ratio K_V/K_B.

Some additional features should be pointed out about (3.6): first, for $\sigma = 1$, one has $K \sim t^{-1}$, a decay rate discussed in Hossain *et al.* (1995), Galtier *et al.* (1997), and which is in agreement with a different approach (Kalelkar & Pandit (2004), equation (11) therein, for $q = 1$, $E \sim k^q$). Furthermore, these theoretical decay exponents are fully consistent with the IK scaling (3.2): indeed, the continuity of the total energy spectrum in $k_L = 1/L$ gives

$$k_L^{\sigma - p + 3/2} \sim \sqrt{\epsilon b_0} \sim \sqrt{\epsilon}(K_B)^{1/4}, \tag{3.7}$$

from which (3.6) directly follows.

In this section, it has been shown that the total energy decays in isotropic MHD similarly to kinetic energy in HIT, with a slight difference due to inverse nonlinear transfers only when $\sigma = 4$. This prediction, assessed numerically, is an important finding of the present work, and strongly differs from the predictions by Galtier *et al.* (1997), essentially because we insisted on the fact that b_0 varies with time, which is a reasonable statement in the absence of a mean magnetic field.

4. Imbalanced isotropic MHD turbulence

In this section, the emphasis is put on the spectral modelling of the velocity–magnetic correlation $\hat{H}_{ij}^c(\boldsymbol{k}) = \langle \hat{u}_i^*(\boldsymbol{k})\hat{b}_j(\boldsymbol{k})\rangle$, which corresponds to $\langle u_i(\boldsymbol{x})b_j(\boldsymbol{x} + \boldsymbol{r})\rangle$ in physical space, with $\boldsymbol{r}$ the separation vector. Some fundamental results about spectral modelling are firstly exposed, and then the nonlinear transfer terms associated with cross-helicity are computed within the EDQNM framework. Finally, numerical results of decaying MHD turbulence with an initial non-zero cross-helicity are presented, i.e. imbalanced isotropic MHD without a mean magnetic field, in order to identify the impact of the cross-correlation on the scalings of $E_B(k, t)$ and $E_V(k, t)$, and on the decay of K. Pressure spectra are addressed as well. It is worth mentioning that such a framework of non-zero cross-helicity without mean magnetic field was also briefly addressed in Wan *et al.* (2012).

4.1. *Modelling of the spectral cross-correlation* $\hat{H}_{ij}^{c}$

Helical decompositions of the spectral fluctuating velocity and magnetic fields are firstly considered, i.e.

$$\hat{u}_i(\boldsymbol{k}) = u_+(\boldsymbol{k})N_i(\boldsymbol{k}) + u_-(\boldsymbol{k})N_i^*(\boldsymbol{k}), \quad \hat{b}_i(\boldsymbol{k}) = b_+(\boldsymbol{k})N_i(\boldsymbol{k}) + b_-(\boldsymbol{k})N_i^*(\boldsymbol{k}), \quad (4.1a,b)$$

where N_i are the helical modes (Cambon & Jacquin 1989) which verify $k_i N_i = 0$, $N_i N_i = 0$ and $N_i(-\boldsymbol{k}) = N_i^*(\boldsymbol{k})$. Because of Hermitian symmetry for $\hat{u}_i$ and $\hat{b}_i$, namely $\hat{u}_i^*(\boldsymbol{k}) = \hat{u}_i(-\boldsymbol{k})$ and $\hat{b}_i^*(\boldsymbol{k}) = \hat{b}_i(-\boldsymbol{k})$, this property is verified as well for the $\pm$ components, $u_\pm^*(\boldsymbol{k}) = u_\pm(-\boldsymbol{k})$ and $b_\pm^*(\boldsymbol{k}) = b_\pm(-\boldsymbol{k})$. Using these decompositions, it directly follows that

$$\begin{aligned}
\hat{H}_{ij}^{c}(\boldsymbol{k}) = {} & \mathcal{H}_c(\boldsymbol{k})P_{ij}(\boldsymbol{k}) + \mathrm{i}\epsilon_{ijn}\alpha_n F^{\mathrm{EM}}(\boldsymbol{k}) \\
& + \langle u_+^*(\boldsymbol{k})b_-(\boldsymbol{k})\rangle N_i^*(\boldsymbol{k})N_j^*(\boldsymbol{k}) + \langle u_-^*(\boldsymbol{k})b_+(\boldsymbol{k})\rangle N_i(\boldsymbol{k})N_j(\boldsymbol{k}),
\end{aligned} \quad (4.2)$$

where the time dependence has been omitted for clarity. The cross-helicity density $\mathcal{H}_c$ is half the trace of the spectral cross-correlation

$$\mathcal{H}_c(\boldsymbol{k}, t) = \tfrac{1}{2}\hat{H}_{ii}^{c}(\boldsymbol{k}, t) = \langle u_+^* b_+\rangle + \langle u_-^* b_-\rangle, \quad (4.3)$$

is real, and verifies $\mathcal{H}_c^*(\boldsymbol{k}) = \mathcal{H}_c(-\boldsymbol{k})$. The cross-helicity K_c is linked to the cross-helical spectrum H_c through

$$K_c(t) = \frac{1}{2}\langle \boldsymbol{u}.\boldsymbol{b}\rangle = \int_0^\infty \int_{S_k} \mathcal{H}_c(\boldsymbol{k}, t)\, \mathrm{d}^2\boldsymbol{k}\, \mathrm{d}k = \int_0^\infty H_c(k, t)\, \mathrm{d}k. \quad (4.4)$$

A non-zero cross-helicity breaks the mirror symmetry of the flow since $\boldsymbol{b}$ is a pseudo-vector, consistently with the decomposition of Frisch *et al.* (1975). Nevertheless, it is possible to consider cross-helicity without magnetic helicity and kinetic helicity.

The second right-hand side term of (4.2) can be non-zero in non-helical turbulence. This term F^{EM} is linked to the cross-correlation through

$$F^{\mathrm{EM}}(\boldsymbol{k}, t) = \langle u_+^* b_+\rangle - \langle u_-^* b_-\rangle = -\tfrac{1}{2}\mathrm{i}\epsilon_{ijl}\alpha_l \hat{H}_{ij}^{c}(\boldsymbol{k}, t). \quad (4.5)$$

The quantity F^{EM} verifies $F^{\mathrm{EM}\,*}(\boldsymbol{k}) = F^{\mathrm{EM}}(-\boldsymbol{k})$. It follows that F^{EM} is linked to the electromotive force through

$$\langle \boldsymbol{u} \times \boldsymbol{b}\rangle = 2\mathrm{i} \int_0^\infty \int_{S_k} \frac{\boldsymbol{k}}{k} F^{\mathrm{EM}}(\boldsymbol{k}, t)\, \mathrm{d}^2\boldsymbol{k}\, \mathrm{d}k = \int_0^\infty \int_{S_k} \epsilon_{pql}\alpha_i\alpha_l \hat{H}_{pq}^{c}(\boldsymbol{k}, t)\, \mathrm{d}^2\boldsymbol{k}\, \mathrm{d}k. \quad (4.6)$$

However, the electromotive force is not considered here in the framework of isotropic MHD turbulence: indeed it would create a mean magnetic field, and thus break the isotropy of the flow, according to

$$\frac{\partial \boldsymbol{B}^0}{\partial t} = \boldsymbol{\nabla} \times \langle \boldsymbol{u} \times \boldsymbol{b}\rangle + \eta\nabla^2\boldsymbol{B}^0. \quad (4.7)$$

The two last right-hand side terms of (4.2) might be non-zero in complex flows such as rotating or sheared MHD turbulence, and may be interpreted as a mixed kinetic-magnetic polarization. But they always vanish in isotropic MHD turbulence

with or without helicity, so that they are discarded from this point. Consequently, the decomposition is similar to the one proposed in Frisch *et al.* (1975), and one has

$$\hat{H}_{ij}^{c}(\boldsymbol{k}) = \hat{H}_{ij}^{c*}(-\boldsymbol{k}) = \mathcal{H}_c(\boldsymbol{k})P_{ij}(\boldsymbol{k}) + i\epsilon_{ijn}\alpha_n F^{\text{EM}}(\boldsymbol{k}). \tag{4.8}$$

In what follows, the spherically averaged equation for the cross-helical spectrum is derived, along with its corresponding spherically averaged nonlinear transfer, and with the additional kinetic and magnetic transfer terms resulting from the presence of $H_c(k, t)$.

4.2. *Equation for the cross-helical spectrum $H_c(k, t)$*

In this part, we derive the evolution equation of the cross-helical spectrum $H_c(k, t)$ in a manner analogous to what was done in §2 for $E_V(k, t)$ and $E_B(k, t)$. Starting from (2.10), and using the modelling of the cross-correlation studied previously, which amounts to $\hat{H}_{ij}^{c} = \mathcal{H}_c P_{ij}$ in IMHDT, yields

$$\left(\frac{\partial}{\partial t} + (\nu + \eta)k^2\right)\mathcal{H}_c(\boldsymbol{k}, t) = \frac{1}{2}T_{ii}^{c}(\boldsymbol{k}, t). \tag{4.9}$$

Then, the EDQNM procedure is applied, and the quasi-normal expressions (2.22) and (2.23) are used to compute explicitly T_{ii}^{c} from (2.16). After classical algebra, this gives the final equation for the cross-helical spectrum

$$\left(\frac{\partial}{\partial t} + (\nu + \eta)k^2\right)H_c(k, t) = S^c(k, t), \tag{4.10}$$

with S^c the spherically averaged cross-helical nonlinear transfer

$$
\begin{aligned}
S^c(k, t) &= \frac{1}{2}\int_{S_k} T_{ii}^{c}(\boldsymbol{k}, t)\mathrm{d}^2\boldsymbol{k} \\
&= 8\pi^2\int_{\Delta_k}\theta_{kpq}k^2pq\left[2k(y^2 - z^2)\mathcal{H}_c''(\mathcal{E}_0^{V'} + \mathcal{E}_0^{B'}) + p\left((xy + z^3)(\mathcal{H}_c''\mathcal{E}_0^B - \mathcal{H}_c\mathcal{E}_0^V)\right.\right. \\
&\quad + (xy + z)(\mathcal{H}_c''\mathcal{E}_0^V - \mathcal{H}_c\mathcal{E}_0^{V''}) + z(1 - y^2)(\mathcal{H}_c''\mathcal{E}_0^B - \mathcal{H}_c\mathcal{E}_0^{B''}) \\
&\quad + \left.\left. z(1 - x^2)(\mathcal{H}_c''\mathcal{E}_0^V - \mathcal{H}_c\mathcal{E}_0^{B''})\right)\right]\mathrm{d}p\,\mathrm{d}q,
\end{aligned}
\tag{4.11}
$$

with $\mathcal{H}_c = H_c(k)/(4\pi k^2)$, $\mathcal{H}_c' = H_c(p)/(4\pi p^2)$ and $\mathcal{H}_c'' = H_c(q)/(4\pi q^2)$. Since the cross-helicity $K_c(t)$ is an inviscid invariant of isotropic MHD turbulence, its nonlinear transfer S^c is conservative, in agreement with the evolution equation

$$\frac{\partial K_c}{\partial t} = -\epsilon_c(t), \quad \epsilon_c(t) = \frac{1}{2}(\nu + \eta)\left\langle\frac{\partial u_i}{\partial x_j}\frac{\partial b_i}{\partial x_j}\right\rangle, \tag{4.12a,b}$$

where ϵ_c is the cross-helicity dissipation rate. Furthermore, according to the quasi-normal expression (2.21), the cross-helical spectrum also impacts the magnetic nonlinear transfers $S^{\text{V(mag)}}$ and $S^{\text{B(mag)}}$. Here are the additional contributions created by a non-zero cross-helicity in the evolution equations of $E_V(k, t)$ and $E_B(k, t)$:

$$S^{\text{V(cross)}}(k, t) = 16\pi^2\int_{\Delta_k}\theta_{kpq}k^2p^2q\mathcal{H}_c''\left[z(1 - y^2)\mathcal{H}_c - (xy + z^3)\mathcal{H}_c'\right]\mathrm{d}p\,\mathrm{d}q, \tag{4.13}$$

$$S^{\text{B(cross)}}(k, t) = 16\pi^2\int_{\Delta_k}\theta_{kpq}k^3pq(1 - y^2 + z^2 + xyz)\mathcal{H}_c''(\mathcal{H}_c - \mathcal{H}_c')\,\mathrm{d}p\,\mathrm{d}q. \tag{4.14}$$

Both $S^{\text{V(cross)}}$ and $S^{\text{B(cross)}}$ are not conservative separately, but the sum has zero integral over the whole wavenumber space. From now on, we write $S^{\text{B}} = S^{\text{B(mag)}} + S^{\text{B(cross)}}$ and $S^{\text{V}} = S^{\text{V(hyd)}} + S^{\text{V(mag)}} + S^{\text{V(cross)}}$. These explicit expressions for the three nonlinear transfers involving the cross-helical spectrum are new. The different contributions of the cross-helical, kinetic and magnetic spectra can be disentangled easily, and this does not prevent us from analysing afterwards E_+ and E_-, linked to the Elsässer variables $z^{\pm} = u \pm b$. On the contrary, in Grappin *et al.* (1982, 1983), the cross-helical transfer terms must be deduced from those associated with E_+ and E_-, with $H_c = (E_+ - E_-)/4$.

At each time and each wavenumber k, the cross-helical spectrum must satisfy the realizability condition given in Frisch *et al.* (1975), namely

$$H_c(k, t) \leqslant \sqrt{E_V(k, t) E_B(k, t)}. \tag{4.15}$$

For the numerical simulations of isotropic imbalanced MHD, we choose $E_V(k, t = 0) = E_B(k, t = 0)$ given by (2.44), with an infrared slope $\sigma = \sigma_B = \sigma_V$ which is either $\sigma = 2$ or $\sigma = 4$. To ensure that (4.15) is always verified, we choose $H_c(k, t = 0) = \sqrt{E_V(k, t=0) E_B(k, t=0)}/c_{\text{cond}}$ with $c_{\text{cond}} = 10$: for smaller values of c_{cond} down to unity, the realizability condition can be violated at large scales after a few turnover times.

It is worth noting that the complete spectral evolution equations of E_V, E_B and H_c are entirely solved numerically unlike in Grappin *et al.* (1982). In the latter reference, reduced equations are obtained with the assumption that equipartition between kinetic and magnetic energy is reached, by imposing a strong mean magnetic field with random orientation to remain statistically isotropic.

In what follows, four different features are addressed in imbalanced IMHDT: the nonlinear transfers, the decay of cross-helicity, the spectral scaling of the main spectra with notably the impact of moderate Reynolds numbers, and finally pressure spectra.

4.3. *Spectral nonlinear transfers in imbalanced MHD*

In this section, we investigate the nonlinear spectral transfers of kinetic energy, magnetic energy and cross-helicity, and their associated fluxes. It is recalled that both $K = K_V + K_B$ and K_c are inviscid invariants of MHD turbulence. To visualize the imbalance of MHD turbulence due to a non-zero cross-correlation $\langle u_i b_i \rangle$, it is convenient to work with the Elsässer spectra

$$E_{\pm}(k, t) = E_V(k, t) + E_B(k, t) \pm 2 H_c(k, t), \quad K_{\pm} = \int_0^{\infty} E_{\pm}(k, t) \, \mathrm{d}k, \tag{4.16a,b}$$

whose integrals over the whole wavenumber space, which we call the Elsässer energies $K_{\pm}$, are inviscid invariants of MHD turbulence as well (in the balanced case, one has $E_+ = E_- = E = E_V + E_B$).

The different fluxes, normalized by the total dissipation rate ϵ, are first presented in figure 5(*a*). The Elsässer, cross-helical and total fluxes Π_+, Π_-, Π^c, and $\Pi^{\text{V}} + \Pi^{\text{B}}$, linked to the inviscid invariants K_+, K_-, K_c and K, are consistently conservative. The $+$ Elsässer flux in slightly more intense than the $-$ one. Moreover, the Elsässer and total fluxes are much stronger than the cross-helical one, which was multiplied by 10 for readability reasons. One can remark that around the integral wavenumber k_L, the cross-helical flux is negative, meaning that part of the cross-helicity is transferred towards large scales. This is not a transient effect, and remains rather subdominant since the main part of the cross-helical flux is positive and constant in the inertial range. This
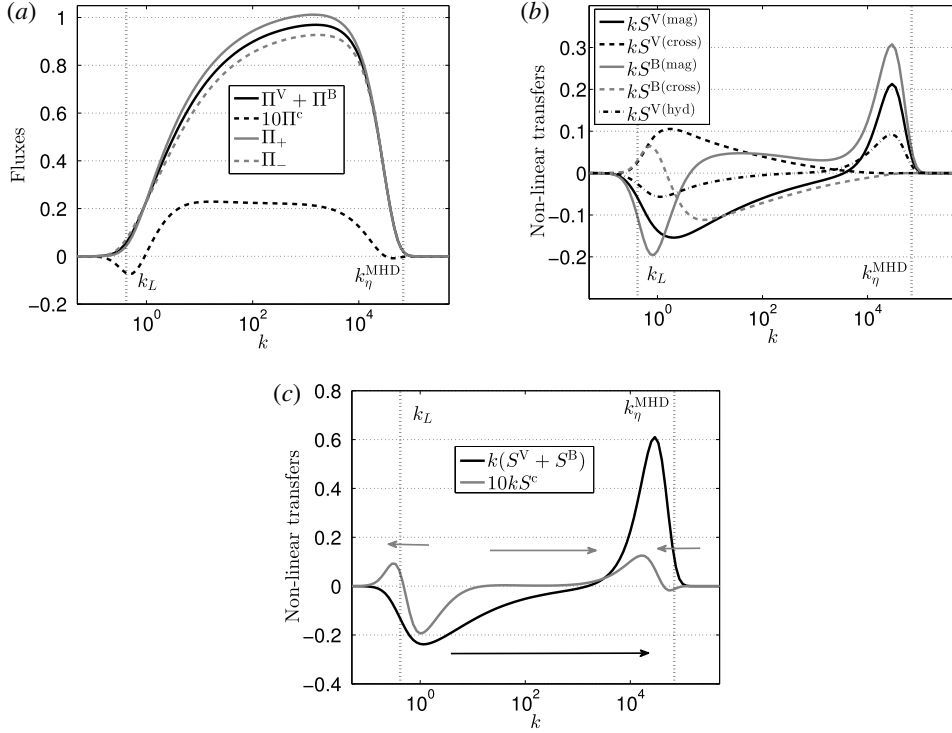
FIGURE 5. Nonlinear transfers and fluxes, normalized by ϵ, at $Re_\lambda(t = 30\tau_0) = 4 \times 10^4$ for $\sigma = 2$, along with the integral and dissipative wavenumbers k_L and k_η^{MHD}. For better readability, the cross-helical transfer and flux were multiplied by 10. (a) Cross-helical flux Π^c, Elsässer fluxes Π_+ and Π_- and total energy flux $\Pi^{\text{V}} + \Pi^{\text{B}}$. ($b$) Kinetic energy transfers (black): $S^{\text{V(hyd)}}$, $S^{\text{V(mag)}}$ and $S^{\text{V(cross)}}$; Magnetic energy transfers (grey): $S^{\text{B(mag)}}$, and $S^{\text{B(cross)}}$. (c) Total transfer $S^{\text{V}} + S^{\text{B}}$ (black) and cross-helical transfer S^c (grey); arrows indicate the direction of the transfers.

could also be a signature of inviscid invariants not positive–definite: indeed, a similar feature was observed for kinetic helicity in HIT (Briard & Gomez 2017).

This is better illustrated in figure 5(b), where the five kinetic and magnetic nonlinear spherically averaged transfers are displayed, namely $S^{\text{V(hyd)}}$, $S^{\text{V(mag)}}$, $S^{\text{V(cross)}}$, $S^{\text{B(mag)}}$ and $S^{\text{B(cross)}}$. These transfer terms can be decomposed into two groups: the ones already present in balanced MHD, $S^{\text{V(hyd)}}$, $S^{\text{V(mag)}}$ and $S^{\text{B(mag)}}$, which are direct transfers from large to small scales. Whereas the terms arising from the presence of cross-helicity, $S^{\text{V(cross)}}$ and $S^{\text{B(cross)}}$, are inverse transfers stronger at large scales, and as intense as the others.

Furthermore, in figure 5(c), the total and cross-helical nonlinear transfers $S^{\text{V}} + S^{\text{B}}$ and S^c are presented. The transfer of total energy is much more intense than the one of cross-helicity: total energy is taken from a large range of scales and brought to smaller scales close to k_η^{MHD}. Whereas S^c is much less intense and transfers cross-helicity in a more complex way: indeed, most of the cross-helicity is taken from a narrow band of large scales to a wide range of smaller scales. But in addition, large scales cross-helicity is also brought at scales bigger than k_L^{-1}, illustrating some strong inverse transfer mechanisms. Moreover, one can observe that around k_η^{MHD}, cross-helicity is

also slightly transferred to larger scales. These different directions of transfers are sketched with arrows in figure 5(*c*).

4.4. *Decay of cross-helicity*

The impact of a non-zero initial cross-helicity on the decay is illustrated in figure 6(*a*): it is shown that with a sufficient initial velocity–magnetic correlation, here for $H_c(k, t = 0) = 0.5\sqrt{E_V(k, t = 0)E_B(k, t = 0)}$, the decay of the total energy K is slightly delayed. If the amount of initial cross-helicity is too weak, there is no visible effect on K. Note that this kind of initial delay is analogous to what was observed in HIT with kinetic helicity (André & Lesieur 1977; Briard & Gomez 2017). Furthermore, during the decay of K_V, K_B and K_c, the normalized correlation $\rho_c = K_c/\sqrt{K_V K_B}$, linked to the averaged cosine of the angle between $\boldsymbol{u}$ and $\boldsymbol{b}$, increases linearly time, from the initial value to unity, meaning toward alignment in the same direction of the velocity and magnetic fields.

The asymptotic decay of cross-helicity is finally briefly discussed. As mentioned above, because of the slow increase of the normalized correlation ρ_c, the realizability condition (4.15) is eventually broken for large times. In other words, this means that long-time decay with several hundreds of turnover times, as in figure 4, cannot be easily performed. Note that this is not a limitation for DNS because in practice only a few turnover times are computed. We nevertheless propose some quantitative information about the decay exponent α_c of cross-helicity, by choosing $K_c(t = 0) = 10^{-2}$, so that a few hundred turnover times occur with the realizability condition satisfied.

Three conclusions can be drawn from figure 6(*b*): (i) the decay of cross-helicity is very slow compared to the decay of total energy; (ii) the decay exponent α_c of K_c seems to be independent of σ, since one has $\alpha_c \simeq -0.2$ for both $\sigma = 2$ and $\sigma = 4$; and (iii) the presence of cross-helicity does not modify the decay exponent of the total energy, since the previous theoretical predictions (3.6) are recovered: see inset of figure 6(*b*) where $\alpha = -1.2$ for $\sigma = 2$ and $\alpha = -1.4$ for $\sigma = 4$. It follows from these three features that the decay of cross-helicity in isotropic MHD is quite different from the decay of kinetic helicity in isotropic hydrodynamic turbulence (Briard & Gomez 2017).

4.5. *The inertial scaling of the cross-helical spectrum $H_c(k, t)$*

In this part, the emphasis is put on the inertial scaling of the cross-helical spectrum $H_c(k, t)$. First, the total energy and cross-helical spectra $E(k, t)$ and $H_c(k, t)$ are presented in figure 7(*a*) for $\sigma = 2$. The inertial scaling of E remains $k^{-3/2}$, similarly to the balanced case: even though not presented, E_V and E_B still scale in $k^{-3/2}$ despite the presence of cross-helicity. The effects of the cross-helicity are more visible on the Elsässer spectra which are discussed in the next section.

The cross-helical spectrum itself scales with a slope close to $k^{-5/3}$, and is negative at small scales, similarly to what was obtained for the kinetic helicity in skew–isotropic turbulence (Briard & Gomez 2017). One could conclude from these observations, at least within the EDQNM framework, that spectra of quantities not positive–definite, such as $\langle \boldsymbol{u} \cdot \boldsymbol{\omega} \rangle$ and $\langle \boldsymbol{u} \cdot \boldsymbol{b} \rangle$, exhibit negative values at small scales, if $\langle \boldsymbol{u} \cdot \boldsymbol{\omega} \rangle$ and $\langle \boldsymbol{u} \cdot \boldsymbol{b} \rangle$ are positive initially.

The present $k^{-5/3}$ scaling is different from the k^{-2} one of Grappin *et al.* (1982): there are at least two arguments to explain the difference, in favour of the present $k^{-5/3}$ inertial range. Firstly, in Grappin *et al.* (1982), as already explained, simplified
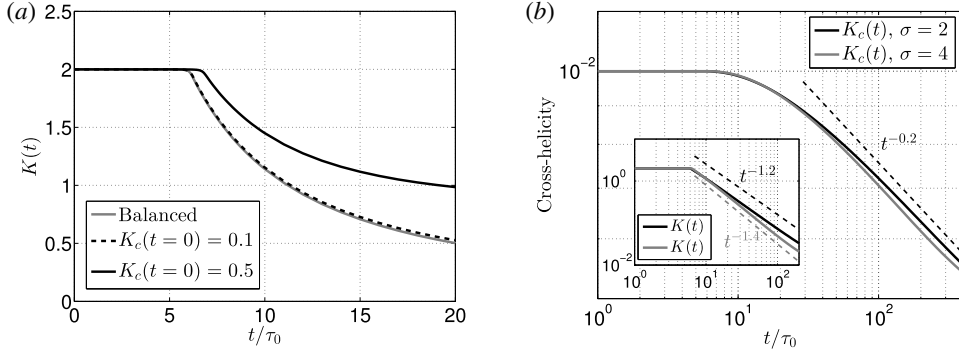
FIGURE 6. Decay of total energy and cross-helicity. (*a*) Impact of initial cross-helicity $K_c(t=0)$ on the early decay of the total energy K compared to the balanced case (in grey) for $\sigma = 2$. (*b*) Long-time decay of cross-helicity with $K_c(t=0) = 10^{-2}$, for $\sigma = 2$ (black) and $\sigma = 4$ (grey); the inset represents the decay of total energy during the same simulation.
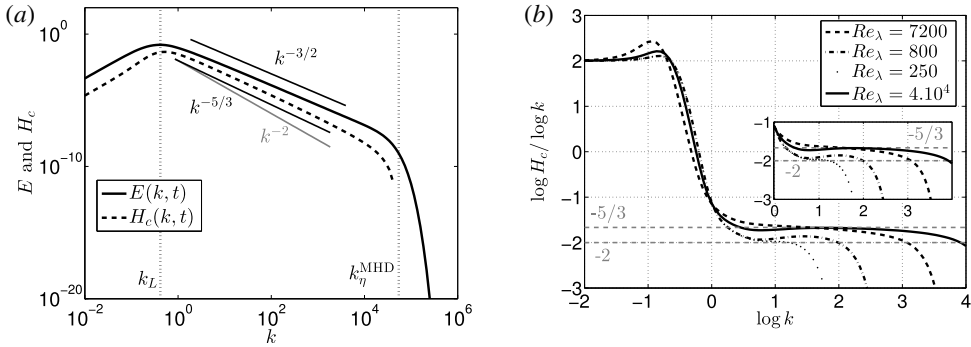

FIGURE 7. Cross-helical spectra for imbalanced MHD for $\sigma = 2$. (*a*) Total energy and cross-helical spectra $E(k,t)$ and $H_c(k,t)$ at $Re_\lambda(t=30\tau_0) = 4 \times 10^4$ along with the integral and dissipative wavenumbers k_L and k_η^{MHD}. (*b*) Spectral slope of H_c, given by $\log H_c / \log k$ for different Re_λ: the $-5/3$ and -2 slopes are indicated in grey; Inset: focus on the inertial range.

EDQNM equations are solved numerically, with the assumption that there is a strong uniform magnetic field of random orientation that causes equipartition of kinetic and magnetic energies, i.e. $E_V = E_B$ at all scales. The difference between the present $k^{-5/3}$ and k^{-2} scalings could thus result from this assumption, but this is rather difficult to quantify. The second argument is a strong Reynolds number effect. In Grappin *et al.* (1982), the Reynolds number is lower than in our case, where $Re_\lambda = 4 \times 10^4$, corresponding to almost two additional decades in wavenumber space. To better illustrate this feature, the slope of H_c for different Re_λ is presented in figure 7(*b*): there is a clear influence of the Reynolds number on the spectral slope of the cross-helical spectrum. Indeed, for moderate $Re_\lambda \sim 250$, the slope of H_c is close to k^{-2}, whereas very large Reynolds numbers are needed to obtain a steady result, close to $k^{-5/3}$ here. Nevertheless, the tendency of our results is in agreement with Grappin *et al.* (1982) regarding the spectral slope of H_c, in a sense that it is steeper than the one of E.

Finally, one can remark that the $-5/3$ slope of the cross-helical spectrum is similar to the one of the kinetic helicity spectrum in HIT, framework in which kinetic helicity is an inviscid invariant, unlike in MHD. If we go further assuming the $k^{-5/3}$ dependence, dimensional analysis provides (i) $H_c(k) \sim \epsilon_c^a \epsilon^b k^{-5/3}$ with $a + b = 2/3$, and $a \neq 0$ since spectra of inviscid invariants are expressed in general as function of their dissipation rate, and (ii) no dependence on b_0. The latter somehow means that the dynamics of H_c becomes much less dependent on the Alfvèn time $\tau_A = (kb_0)^{-1}$, which is consistent with the cross-helicity reducing initially the nonlinear transfers, as shown in figure 6(*a*). Compensating H_c with the different possibilities for a and b indicates that a relevant scaling could be

$$H_c(k, t) = C_c \, (\epsilon \epsilon_c)^{1/3} \, k^{-5/3}, \qquad (4.17)$$

which gives $C_c \simeq 3$, similar to the value of C_{IK} for E. Choosing a 'linear' dependency on ϵ_c ($a = 1$ and $b = -1/3$) yields a way too large constant compared to other usual constants ($C_c \geqslant 30$): the fact that H_c should not depend linearly on ϵ_c is consistent with some arguments proposed by Grappin *et al.* (1982).

Now that the inertial scaling of H_c has been addressed and the impact of moderate Reynolds numbers highlighted, the effects of cross-helicity on the Elsässer spectra and on the short-time dynamics are analysed.

4.6. E_+, E_- and the short-time dynamics

It has been shown in figure 6(*a*) that a sufficient amount of initial cross-helicity $K_c(t = 0)$ could slightly delay the initial decay of total energy K, a feature similar to what is obtained in HIT with initial kinetic helicity (André & Lesieur 1977). Furthermore, it was revealed in the previous section that the presence of cross-helicity was not changing the inertial scaling of the kinetic, magnetic and total spectra E_V, E_B and $E = E_V + E_B$. Therefore, it is proposed in this part to briefly illustrate the impact of cross-helicity on the inertial scalings of the Elsässer spectra E_+ and E_- defined in (4.16), and on the short-time dynamics as well.

One can observe in figure 8(*a*) that adding a greater amount of initial cross-helicity tends to increase the kinetic to magnetic energy ratio K_V/K_B, along with the positive Elsässer energy K_+, the latter being expected from the definition (4.16). Some justification are proposed hereafter to justify the increase of kinetic energy by adding cross-helicity in the flow. Regarding the asymptotic value of K_V/K_B for the balanced case, it is worth noting that it is rather independent of the Reynolds number and only slightly depends on the initial conditions (see figure 11(*d*) in appendix A.2 for more details).

The Elsässer spectra E_+ and E_- are presented in figure 8(*b*). Unlike for E_V, E_B and E, a slight departure is observed for their inertial scaling with respect to the IK prediction in $k^{-3/2}$: the spectral slope of E_+ is steeper, between $k^{-1.55}$ and $k^{-5/3}$, whereas the opposite happens for E_-, where the slope is approximately between $k^{-1.2}$ and $k^{-4/3}$. It is rather difficult to determine the exact scalings of E_+ and E_- since the inertial slopes slightly vary with both $K_c(t = 0)$ and the Reynolds number. Nevertheless, the finding that the slope of E_+ becomes steeper than $-3/2$ and the one of E_- less steep is a robust feature, already obtained in Grappin *et al.* (1982). In fact, even though equipartition is not assumed here unlike the latter reference, the inertial spectral slopes obtained for $E_+ \sim k^{-m_+}$ and $E_- \sim k^{-m_-}$ are in agreement with the prediction of Grappin and coworkers, namely $m_+ + m_- \simeq 3$.
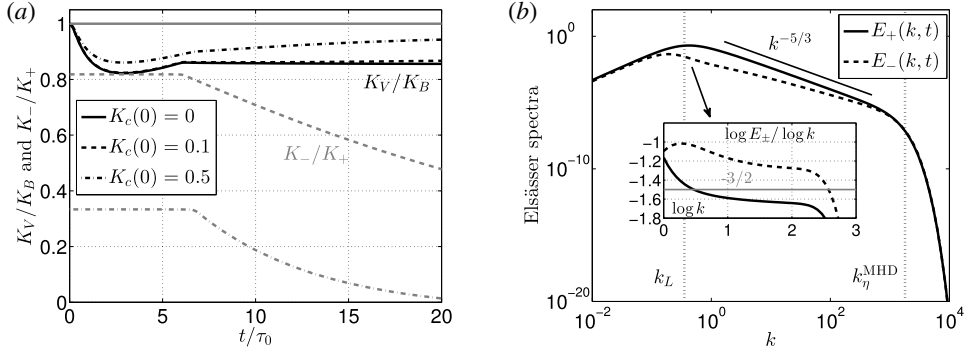
FIGURE 8. (*a*) Impact of the initial cross-helicity $K_c(t=0)$ on the short-time dynamics, for $\sigma = 2$ and $E_V(k, t=0) = E_B(k, t=0)$, on the ratios K_V/K_B (black) and K_-/K_+ (grey). (*b*) Elsässer spectra E_+ and E_-, for $\sigma = 2$ and $Re_\lambda(t = 30\tau_0) = 2 \times 10^3$, with initial condition $H_c(k, t=0) = 0.1\sqrt{E_V(k, t=0)E_B(k, t=0)}$; The inset gives the slope $\log E_\pm / \log k$ in the inertial range.

Now, we wish to interpret physically the meaning of the departure of E_+ and E_- from the IK $k^{-3/2}$ scaling. It is clear from figure 8(*b*) that the Elsässer spectrum E_+ is the most intense, consistently with the fluxes displayed earlier in figure 5(*a*). In terms of the Elsässer variables $z^\pm = u \pm b$, it means that adding some positive $\langle u \cdot b \rangle$ in the flow enhances the dynamics of z^+, thus making E_- less intense than E_+. Therefore, z^+ is transported by a subdominant field at large scales, leading to a Kolmogorov-like local transfer mechanism for E_+, with the characteristic time $\tau_V = (\epsilon k^2)^{-1/3}$ like in HIT. This further justifies that the scaling of E_+ tends to $k^{-5/3}$. On the contrary, since the transport of z^- is amplified, the 'Alfvénization' phenomenon is increased for E_- and the nonlinear transfers are slowed down, thus explaining the slope less steep than $-3/2$, close to $E_- \sim k^{-4/3}$. Incidentally, the fact that the Kolmogorov-type dynamics is dominant (because $E_+ > E_-$ at the most energetic scales) is consistent with the growth of the kinetic to magnetic energy ratio in figure 8(*a*), and with the phenomenology of Dobrowolny, Mangeney & Veltri (1980) as well, where E_+ should prevail if positive cross-correlation is initially dominant.

Based on these observations, one could propose theoretical scalings for the Elsässer spectra in imbalanced IMHDT. Proceeding as in § 3.1, one would have $\epsilon_+ = kE_+(k)/\tau_V(k)$ so that $E_+ \sim \epsilon_+\epsilon^{-1/3}k^{-5/3}$ and $\epsilon_- = kE_-/\tau_{\mathrm{tr}}(k)$ with $\tau_{\mathrm{tr}}(k) = (k^2\epsilon)^{-2/3}/(kb_0)^{-1}$ so that $E_- \sim \epsilon_-b_0\epsilon^{-2/3}k^{-4/3}$.

The conclusion is that cross-helicity affects both the early dynamics of the decaying turbulent flow, and the inertial scalings of the Elsässer spectra as well, with different mechanisms at stake for E_+ and E_-. If one injects instead negative correlation $\langle u \cdot b \rangle$, the previous findings are still verified by changing the $()_+$ and $()_-$ quantities. The $k^{-5/3}$ and $k^{-4/3}$ scalings for E_+ and E_- respectively deserve more investigation, since two different effects are in competition: a larger Reynolds number which brings the slopes closer to $k^{-3/2}$, and a greater normalized cross-helicity ρ_c which on the contrary makes the slopes depart from $k^{-3/2}$.

4.7. *Pressure spectrum $E_P(k, t)$*

Now that the impact of cross-helicity on the kinetic energy, magnetic energy, and Elsässer spectra has been discussed, the emphasis is put here on pressure spectra.

The evolution equation of the pressure fluctuations, the so-called Poisson equation, is obtained by taking the divergence of the velocity fluctuations equation (2.1)

$$-\frac{\partial^2 p^*}{\partial x_j \partial x_j} = \frac{\partial u_j}{\partial x_i}\frac{\partial u_i}{\partial x_j} - \frac{\partial b_j}{\partial x_i}\frac{\partial b_i}{\partial x_j}. \tag{4.18}$$

The spectral two-point second-order pressure correlation is then defined as

$$\mathcal{E}_P(\boldsymbol{k}, t)\delta(\boldsymbol{k} - \boldsymbol{p}) = \langle \hat{p}(\boldsymbol{k}, t)\hat{p}^*(\boldsymbol{p}, t)\rangle, \tag{4.19}$$

where the spectral fluctuating pressure is given by

$$\hat{p}(\boldsymbol{k}, t) = \alpha_i\alpha_j\left(\widehat{b_ib_j}(\boldsymbol{k}, t) - \widehat{u_iu_j}(\boldsymbol{k}, t)\right). \tag{4.20}$$

The spectral second-order pressure correlation reads, after some algebra,

$$\mathcal{E}_P(\boldsymbol{k}) = 2\alpha_i\alpha_j\alpha_p\alpha_q \int_{\boldsymbol{k}=\boldsymbol{p}+\boldsymbol{q}} \left[\hat{R}_{ip}(\boldsymbol{p})\hat{R}_{jq}(\boldsymbol{q}) + \hat{B}_{ip}(\boldsymbol{p})\hat{B}_{jq}(\boldsymbol{q}) - 2\Re\left(\hat{H}_{ip}^c(\boldsymbol{p})\hat{H}_{jq}^c(\boldsymbol{q})\right)\right]\,\mathrm{d}^3\boldsymbol{p}. \tag{4.21}$$

The pressure spectrum, obtained by spherically averaging $\mathcal{E}_P$, is then

$$\begin{aligned}
E_P(k, t) &= \int_{S_k}\mathcal{E}_P(\boldsymbol{k}, t)\,\mathrm{d}^2\boldsymbol{k} = E_P^{(\mathrm{hyd})}(k, t) + E_P^{(\mathrm{mag})}(k, t) + E_P^{(\mathrm{cross})}(k, t)\\
&= 16\pi^2\int_{\Delta_k} kpq(1 - y^2)(1 - z^2)(\mathcal{E}_0^{V'}\mathcal{E}_0^{V''} + \mathcal{E}_0^{B'}\mathcal{E}_0^{B''})\,\mathrm{d}p\,\mathrm{d}q\\
&\quad - 32\pi^2\int_{\Delta_k} kpq(1 - y^2 - z^2 + y^2z^2)\mathcal{H}_c'\mathcal{H}_c''\,\mathrm{d}p\,\mathrm{d}q,
\end{aligned} \tag{4.22}$$

where $E_P^{(\mathrm{hyd})}$ is the classical pressure spectrum of HIT (Meldi & Sagaut 2013*b*; Briard, Iyer & Gomez 2017), $E_P^{(\mathrm{mag})}$ is the additional contribution in MHD resulting from the Laplace force and $E_P^{(\mathrm{cross})}$ corresponds to the impact of cross-helicity. In the following simulations, the pressure spectrum is set to zero initially: it is always found that the infrared scaling is k^2, as in HIT (Lesieur *et al.* 1999).

In balanced MHD (with $E_P^{(\mathrm{cross})} = 0$), it follows that the scaling of the pressure spectrum is different from its $k^{-7/3}$ inertial scaling in HIT: indeed, by dimensional analysis, one obtains $E_P \sim kE_B(k)^2 \sim kE_V(k)^2$, so that

$$E_P(k, t) \sim b_0\,\epsilon\,k^{-2}. \tag{4.23}$$

This k^{-2} inertial scaling is assessed in figure 9(*a*) for $E_P^{(\mathrm{mag})}$ and $E_P^{(\mathrm{iso})}$, and thus for E_P as well. One can remark that at large scales, $E_P^{(\mathrm{mag})}$ is more intense than $E_P^{(\mathrm{hyd})}$: this is because of the initial conditions (2.44), where $E_B \sim k^2$ and $E_V \sim k^4$ at large scales. Note that the pressure variance, defined as $K_P = \int_0^\infty E_P(k)\,\mathrm{d}k$, decays at a rate 2α, with $K \sim t^\alpha$, for dimensional reasons since $p^2 \sim u^4$, similarly to HIT (Meldi & Sagaut 2013*b*).

For imbalanced MHD, if an inertial $k^{-5/3}$ scaling is assumed for the cross-helical spectrum, as shown previously in figure 7(*a*), it follows that $E_P^{(\mathrm{cross})} \sim kH_c(k)^2 \sim k^{-7/3}$: this scaling is recovered here in figure 9(*b*), and one can observe that $E_P^{(\mathrm{cross})}$ is mainly negative, which is expected given its expression (4.22). Other possible effects of cross-helicity on the hydrodynamic and MHD parts are rather difficult to quantify, since the scaling of $E_P^{(\mathrm{mag})}$ and $E_P^{(\mathrm{iso})}$ remains like k^{-2}.
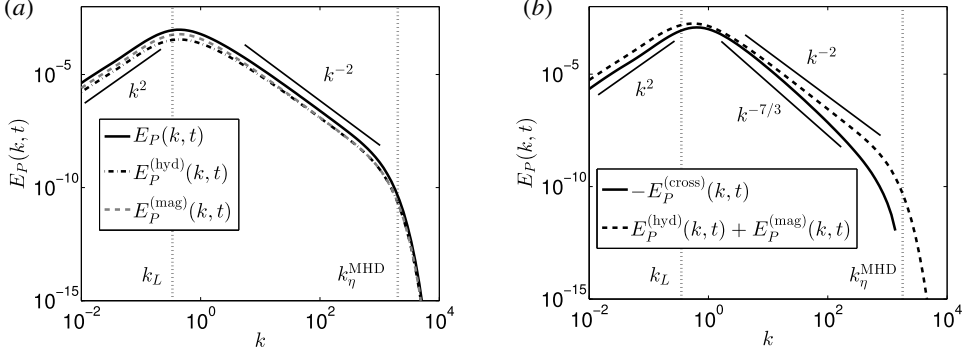
FIGURE 9. Pressure spectra for balanced and imbalanced isotropic MHD, for $\sigma = 2$ at $Re_\lambda = 3 \times 10^3$, along with the integral and dissipative wavenumbers k_L and k_η^{MHD}, with initial condition $E_B(k, t = 0) = E_V(k, t = 0)$. (a) Balanced case: $E_P(k, t)$ with its isotropic and magnetic parts $E_P^{(\mathrm{hyd})}(k, t)$ and $E_P^{(\mathrm{mag})}(k, t)$. (b) Imbalanced case: $E_P^{(\mathrm{hyd})}(k, t)$, $E_P^{(\mathrm{mag})}(k, t)$ and $E_P^{(\mathrm{cross})}(k, t)$.

5. Assessment of the $4/3$rd laws for isotropic MHD

In this part, we focus on statistics of homogeneous isotropic balanced and imbalanced MHD turbulence. The objective is to assess the two $4/3$rd laws for the total energy and cross-helicity. Note that some calculations and simplifications are proposed in appendices B.1 and B.2 regarding the evolution equation of the total dissipation rate ϵ.

We aim at assessing at large Reynolds numbers in both decaying balanced and imbalanced IMHDT the asymptotic $4/3$rd laws for structure functions, derived in Politano & Pouquet (1998*a*), namely

$$D^{(\mathrm{MHD})} = \langle \delta u_L(\delta u_i \delta u_i + \delta b_i \delta b_i) - 2\delta b_L \delta u_i \delta b_i \rangle = -\tfrac{4}{3}r\epsilon, \tag{5.1}$$

$$D_c^{(\mathrm{MHD})} = \langle \delta u_L \delta u_i \delta b_i \rangle - \tfrac{1}{2}\langle \delta b_L(\delta b_i \delta b_i + \delta u_i \delta u_i) \rangle = -\tfrac{4}{3}r\epsilon_c, \tag{5.2}$$

where r is the distance between two points located in $\boldsymbol{x}$ and $\boldsymbol{x}' = \boldsymbol{x} + \boldsymbol{r}$, the subscript $()_L$ refers to the component along $\boldsymbol{r}$, the prime $'$ to quantities expressed in $\boldsymbol{x}'$ and the increment is defined as $\delta u_i = u_i' - u_i$. The second scaling (5.2) is specific to imbalanced MHD, whereas the first one (5.1) is supposed to be verified in both imbalanced and balanced MHD. One can remark that the definition of $D_c^{(\mathrm{MHD})}$ differs from Politano & Pouquet (1998*a*): indeed, here cross-helicity is defined as $\langle u_i b_i \rangle / 2$ and not $\langle u_i b_i \rangle$. The term $\langle \delta b_L \delta u_i \delta b_i \rangle$ is linked to the coupling between the equations for the velocity and magnetic fields, and is non-zero even without cross-helicity.

In order to assess at large Reynolds numbers these two expressions, we need to derive formulae which allow us to compute $D^{(\mathrm{MHD})}$ and $D_c^{(\mathrm{MHD})}$ from the spectral nonlinear transfers. The evolution equations of the kinetic, magnetic and cross-helical structure functions $\langle \delta u_i \delta u_i \rangle$, $\langle \delta b_i \delta b_i \rangle$ and $\langle \delta u_i \delta b_i \rangle$ read

$$\frac{\partial \langle \delta u_i \delta u_i \rangle}{\partial t} + \frac{\partial \langle \delta u_j \delta u_i \delta u_i \rangle}{\partial r_j} = 2\nu \frac{\partial^2 \langle \delta u_i \delta u_i \rangle}{\partial r_j \partial r_j} - 4\epsilon_V + 2\left\langle \delta u_i \delta b_j \frac{\partial \delta b_i}{\partial r_j} \right\rangle, \tag{5.3}$$

$$\frac{\partial \langle \delta b_i \delta b_i \rangle}{\partial t} + \frac{\partial \langle \delta u_j \delta b_i \delta b_i \rangle}{\partial r_j} = 2\eta \frac{\partial^2 \langle \delta b_i \delta b_i \rangle}{\partial r_j \partial r_j} - 4\epsilon_B + 2\left\langle \delta b_i \delta b_j \frac{\partial \delta u_i}{\partial r_j} \right\rangle, \tag{5.4}$$

$$\frac{\partial \langle \delta u_i \delta b_i \rangle}{\partial t} + \frac{\partial \langle \delta u_j \delta b_i \delta u_i \rangle}{\partial r_j} = 2\nu \frac{\partial^2 \langle \delta u_i \delta b_i \rangle}{\partial r_j \partial r_j} - 4\epsilon_c + \frac{1}{2}\frac{\partial}{\partial r_j}\langle \delta b_j(\delta b_i \delta b_i + \delta u_i \delta u_i)\rangle. \quad (5.5)$$

For the latter equation (5.5), a unit magnetic Prandtl number ($\nu = \eta$) was assumed for simplicity. Summing (5.3) and (5.4), and further neglecting the time derivative along with the viscous terms, negligible in the inertial range at large Reynolds numbers, one gets

$$\frac{\partial}{\partial r_j}\left(\langle \delta u_j(\delta u_i \delta u_i + \delta b_i \delta b_i) - 2\delta b_j \delta u_i \delta b_i\rangle\right) = -4\epsilon. \quad (5.6)$$

The final step consists into writing $\delta u_j = r_j \delta u_L / r$, and using $\partial_{r_j}(r_j D^{(\mathrm{MHD})}/r) = \partial_r(r^2 D^{(\mathrm{MHD})})/r^2$, so that integration yields (5.1). Proceeding similarly with (5.5) allows us to recover (5.2).

To obtain a relation between spectral and physical quantities, additional equations are needed. We define the two-point kinetic, magnetic and cross-helical correlations in physical space

$$R_{ij}(r, t) = \langle u_i u_j' \rangle, \quad B_{ij}(r, t) = \langle b_i b_j' \rangle, \quad H_{ij}(r, t) = \langle u_i b_j' \rangle, \quad (5.7a\text{--}c)$$

along with the scalar quantities $2R(r) = \langle u_i u_i' \rangle$, $2B(r) = \langle b_i b_i' \rangle$ and $2H(r) = \langle u_i b_i' \rangle$, which are linked to the previous structure functions through $\langle \delta u_i \delta u_i \rangle = 4K_V - 4R$, and similarly for the magnetic field and the cross-helicity. The evolution equations of R, B and H thus read

$$\frac{\partial R}{\partial t} = \frac{2\nu}{r^2}\frac{\partial}{\partial r}\left(r^2 \frac{\partial R}{\partial r}\right) + \frac{\partial}{\partial r_l}\langle u_i u_l u_i' - b_i b_l u_i' \rangle, \quad (5.8)$$

$$\frac{\partial B}{\partial t} = \frac{2\eta}{r^2}\frac{\partial}{\partial r}\left(r^2 \frac{\partial B}{\partial r}\right) + \frac{\partial}{\partial r_l}\langle u_l b_i b_i' - u_i b_l b_i' \rangle, \quad (5.9)$$

$$\frac{\partial H}{\partial t} = \frac{(\nu + \eta)}{r^2}\frac{\partial}{\partial r}\left(r^2 \frac{\partial H}{\partial r}\right) + \frac{1}{2}\frac{\partial}{\partial r_l}\langle u_i u_l b_i' - b_i b_l b_i' + u_l b_i u_i' - b_l u_i u_i' \rangle, \quad (5.10)$$

which were notably obtained in Chandrasekhar (1951). Summing the two first equations, and using the previous relations yields

$$-4\epsilon - \frac{\partial}{\partial t}\langle \delta u_i \delta u_i + \delta b_i \delta b_i \rangle = \frac{8}{r^2}\frac{\partial}{\partial r}\left(r^2 \frac{\partial}{\partial r}(\nu R + \eta B)\right)$$
$$+ 4\frac{\partial}{\partial r_l}\langle \underbrace{u_i u_l u_i' - b_i b_l u_i'}_{(i)} + \underbrace{u_l b_i b_i' - u_i b_l b_i'}_{(ii)} \rangle. \quad (5.11)$$

Dropping the time derivative and viscous terms, and further identifying with (5.6) gives that $\partial_r(r^2 D^{(\mathrm{MHD})}) = 4r^2 \partial_{r_l}\langle (i) + (ii)\rangle$. Proceeding similarly with the equation of H, and identifying with the equations of $E_V + E_B$ and H_c, finally yields

$$D^{(\mathrm{MHD})}(r, t) = \int_0^\infty \frac{4}{k}\left(S^{\mathrm{V}}(k, t) + S^{\mathrm{B}}(k, t)\right)\left[\frac{\sin(kr)}{(kr)^2} - \frac{\cos(kr)}{kr}\right] dk, \quad (5.12)$$

$$D_c^{(\mathrm{MHD})}(r, t) = \int_0^\infty \frac{4}{k}S^c(k, t)\left[\frac{\sin(kr)}{(kr)^2} - \frac{\cos(kr)}{kr}\right] dk, \quad (5.13)$$
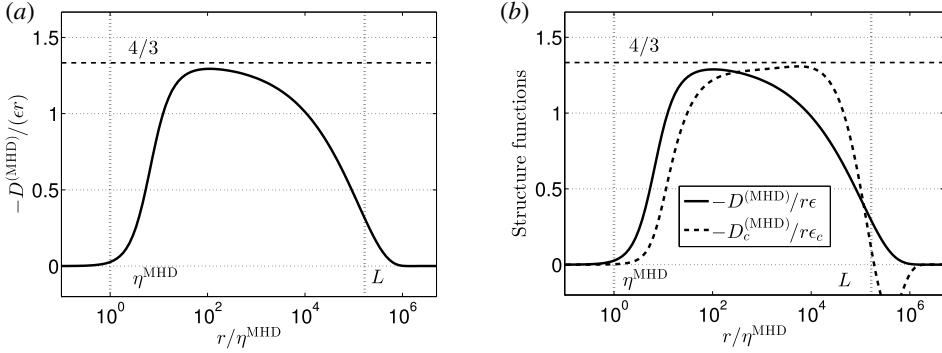
FIGURE 10. Compensated structure functions for balanced and imbalanced MHD turbulence for $\sigma = 2$, along with the integral and dissipative scales L and η^{MHD}. (a) $-D^{\text{MHD}}/(\epsilon r)$ at $Re_\lambda = 2 \times 10^4$. (b) $-D^{\text{MHD}}/(\epsilon r)$ and $-D_c^{\text{MHD}}/(\epsilon_c r)$ at $Re_\lambda = 4 \times 10^4$.

and these formulae are completely analogous to the ones used for kinetic and helical structure functions in isotropic turbulence (Briard & Gomez 2017). Some details about the (i) and (ii) terms are given in appendix B.3, along with their link to the 4/5th law for balanced isotropic MHD turbulence.

The spectral-to-physical space formulae (5.12) and (5.13) are used to assess the 4/3rd laws of balanced and imbalanced MHD turbulence in figure 10(a,b). First, for the fully isotropic case in figure 10(a) at $Re_\lambda = 2 \times 10^4$, there is a satisfactory agreement for the compensated structure function with the expected value 4/3, comparable to recent results in HIT (Briard & Gomez 2017). The difference is attributed to the non-stationarity since the turbulence is not forced in the present simulations. Secondly, for the case with cross-helicity in figure 10(b) at $Re_\lambda = 4 \times 10^4$, the agreement with the expected 4/3 is satisfactory as well. A noteworthy feature is that $-D_c^{(\text{MHD})}/r\epsilon_c$ tends to 4/3 at inertial scales slightly larger than the ones for which $-D^{(\text{MHD})}/r\epsilon$ tends to 4/3. In addition, unlike the structure function of total energy, the cross-helical structure functions is negative at scales larger than the integral one L. For both the balanced and imbalanced cases, there is less than 3 % departure from the theoretical prediction 4/3, derived for infinite Reynolds numbers and stationary turbulence.

The 4/3rd laws for total energy and cross-helicity were assessed numerically here in decaying isotropic MHD turbulence within 3 %. This slight departure from the expected 4/3 is due to the non-stationarity, and not to the inertial scalings of the spectra. Indeed, both the IK $k^{-3/2}$ inertial scaling of the total energy spectrum and the Kolmogorov $k^{-5/3}$ inertial scaling of the cross-helical spectrum are compatible with the 4/3rd scaling of the third-order structure functions.

6. Conclusion and perspectives

In this work, decaying isotropic MHD turbulence (IMHDT) was investigated numerically at large Reynolds numbers using EDQNM, without any background mean magnetic field, as done in the pioneering study of Pouquet *et al.* (1976). Within the EDQNM modelling, an eddy-damping term μ_A is added to take into account the interactions of Alfvén waves packets and ensure realizability. Consequently, since μ_A^{-1} becomes the characteristic time of the inertial range, the total energy spectrum $E(k, t)$ follows the $k^{-3/2}$ Iroshnikov–Kraichnan (IK) scaling. Therefore, the objective

of this work is not to analyse if the inertial scaling is $k^{-3/2}$ or $k^{-5/3}$ since it is prescribed by the modelling, but rather to analyse the decay of total energy, and the impact of cross-helicity on the global dynamics. The overall purpose of this work was also to propose a solid basis for future works in anisotropic MHD turbulence, in order to further disentangle the complex interactions between the different fields at stake. The first part dealt with balanced MHD, in which cross-helicity is zero; in the second part, cross-helicity was initially injected in the flow at large scales; and in the last part, statistics were addressed in physical space.

For balanced IMHDT, the total, kinetic and magnetic energy spectra verify the IK scaling, namely $E \sim E_V \sim E_B \sim k^{-3/2}$: the different kinetic and magnetic nonlinear transfers exchange energy from large to small scales, and no significant inverse cascades mechanisms were found. The residual energy spectrum E_R was investigated in appendix A as well for various initial conditions. The main original contribution is the prediction of the long-time decay of the total energy K at large Reynolds numbers as a function of the large scale infrared slope σ. A new theoretical time exponent α is derived, with $K \sim t^\alpha$, which is interestingly the same as the one of kinetic energy in HIT (Lesieur 2008; Meldi & Sagaut 2013a), and assessed numerically. It is worth noting that an inertial scaling in $k^{-3/2}$ is compatible with a decay rate of the total energy similar to the decay rate of kinetic energy in isotropic hydrodynamic turbulence, the framework in which the kinetic energy spectrum scales as $k^{-5/3}$. Our prediction is at variance with Galtier *et al.* (1999), where the root mean square of the magnetic energy b_0 is assumed to be constant. Hence, we believe that the prediction of the latter reference should be more adapted to strong MHD with a mean magnetic field, when the turbulent transfers occur mainly in the plane perpendicular to $\boldsymbol{B}^0$. This needs to be verified by three-dimensional DNS, a rather complex task since a great number of turnover times is required.

In a second part, an initial non-zero cross-helicity $\langle \boldsymbol{u} \cdot \boldsymbol{b} \rangle$ was injected at large scales to better understand what are the effects of the velocity–magnetic correlation on the spectral scalings and dynamics, still without a mean magnetic field to discard considerations about the anisotropy of the flow. We derived a complete spectral modelling for the cross-helicity, which reduces to the expression of Frisch *et al.* (1975) for IMHDT. In particular, the velocity–magnetic correlation can contain effects from the electromotive force, and more subtle anisotropic features possibly present in rotating or shear MHD turbulence. Beyond these theoretical considerations, three effects of cross-helicity can be highlighted: (i) the initial reduction of nonlinear transfers, similarly to the effect of kinetic helicity in HIT (Briard & Gomez 2017); (ii) the increase of the kinetic to magnetic energy ratio with larger amount of positive initial $\langle \boldsymbol{u} \cdot \boldsymbol{b} \rangle$; and (iii) the fact that K_c decays much slowly than K, with a decay exponent close to -0.2 very likely independent of the large scale infrared slope σ.

The important and original result of this section is that the cross-helical spectrum H_c experiences a significant effect from moderate Reynolds numbers in the inertial range. Indeed, it scales as $H_c \sim k^{-5/3}$ for large Re_λ only, whereas for lower Re_λ, a transient scaling close to k^{-2} is found. Consequently, moderate Reynolds numbers effects explain the difference between the present $H_c \sim k^{-5/3}$ scaling and the $H_c \sim k^{-2}$ proposed by Grappin *et al.* (1982). Moreover, it was shown numerically that despite the presence of cross-helicity, the spectra E, E_V and E_B still scale in $k^{-3/2}$ in the present work. The net effect of the velocity–magnetic correlation can be observed through the Elsässer spectra E_+ and E_-, which both depart from the $k^{-3/2}$ IK scaling. More precisely, it seems that with enough cross-helicity, the Elsässer spectra slowly approach $E_+ \sim k^{-5/3}$ and $E_- \sim k^{-4/3}$, because the dynamics of E_+ becomes

Kolmogorov-like, with a characteristic time $(k^2\epsilon)^{-1/3}$, whereas the 'Alfvénization' is enhanced for E_-, thus slowing down even more the transfers. Some work still needs to be done to determine what should be the final scalings of the $E_\pm$ spectra, since they depend on both the relative level of cross-helicity, which increases with time, and the Reynolds number. The important conclusion nevertheless remains that cross-helicity does not make the total, kinetic and magnetic energy spectra deviate from the $k^{-3/2}$ scaling in the isotropic framework, only the Elsässer spectra.

A subsequent theoretical analysis, made rather simple thanks to EDQNM, is to address pressure fluctuations due to the magnetic field in the Poisson equation. It is found that for the total pressure spectrum, the usual hydrodynamic part depending on E_V and the magnetic part depending on E_B both scale in k^{-2} in the inertial range, whereas the subdominant cross-helical part behaves like $k^{-7/3}$ for the imbalanced case.

Finally, in physical space, the two 4/3rd laws for the total energy and the cross-helicity were assessed numerically with good agreement, at large Reynolds numbers, in decaying MHD turbulence. A noteworthy feature to underline is that both the total energy and the cross-helicity are equally close to the 4/3rd prediction, whereas $E(k, t)$ and $H_c(k, t)$ scale respectively in the inertial range as $k^{-3/2}$ and $k^{-5/3}$. Some developments were proposed in appendix to simplify the evolution equation of the total dissipation rate.

The most important and relevant perspective of this work would be to derive a three-dimensional anisotropic EDQNM model, with $\mathbf{k}$-dependence, to analyse the anisotropy created by a mean magnetic field at large Reynolds number and possibly to shed some light on the $k_\perp^{-3/2}$ versus $k_\perp^{-5/3}$ controversial topic. All the ingredients are available: the theoretical features for a $\mathbf{k}$-dependent anisotropic EDQNM model (Cambon *et al.* 1997), and the anisotropic modelling of homogeneous and solenoidal tensors (Briard, Gomez & Cambon 2016), to be extended to the magnetic field.

Appendix A. Additional results in spectral space

In this section, some complementary results are gathered: first, some considerations about the modelling of the magnetic potential spectrum are proposed. Then, numerical results about the residual spectrum E_R are presented.

A.1. *Magnetic potential spectrum $A(k, t)$*

In this part, it is proposed to briefly analyse the modelling of the magnetic potential spectrum $A(k, t)$. This is of theoretical interest since its nonlinear spectral transfer is linked to the third-order correlation $\langle aub \rangle$: this correlation, written symbolically, was examined in Politano, Gomez & Pouquet (2003), and it was notably shown that in the inviscid case, it is exactly related to the dissipation rate of the magnetic helicity.

The evolution equation of the magnetic potential $\mathbf{a}$, defined as $\mathbf{b} = \nabla \times \mathbf{a}$, with the Coulomb Gauge $\nabla \cdot \mathbf{a} = 0$ to make it divergence free, reads

$$\frac{\partial \mathbf{a}}{\partial t} = \mathbf{u} \times \mathbf{b} + \eta \nabla^2 \mathbf{a}. \tag{A 1}$$

One can define a two-point second-order spectral tensor for the magnetic potential as

$$\hat{A}_{ij}(\mathbf{k}, t)\delta(\mathbf{k} - \mathbf{p}) = \langle \hat{a}_i^*(\mathbf{p}, t)\hat{a}_j(\mathbf{k}, t) \rangle, \tag{A 2}$$

whose evolution equation is

$$\left(\frac{\partial}{\partial t} + 2\eta k^2 \right) \hat{A}_{ij}(\mathbf{k}, t) = T_{ij}^A(\mathbf{k}, t). \tag{A 3}$$

The associated nonlinear transfer reads

$$T_{ij}^{A}(\boldsymbol{k}, t) = \epsilon_{imn} \int S_{njm}^{aub}(\boldsymbol{k}, \boldsymbol{p}, t)\, \mathrm{d}^3\boldsymbol{p} + \epsilon_{jmn} \int S_{nim}^{aub*}(\boldsymbol{k}, \boldsymbol{p}, t)\, \mathrm{d}^3\boldsymbol{p}, \tag{A 4}$$

where S_{ijl}^{aub} is the following three-point third-order spectral correlation

$$S_{ijl}^{aub}(\boldsymbol{k}, \boldsymbol{p}, t)\delta(\boldsymbol{k} + \boldsymbol{p} + \boldsymbol{q}) = \langle \hat{b}_i(\boldsymbol{q}, t)\hat{a}_j(\boldsymbol{k}, t)\hat{u}_l(\boldsymbol{p}, t)\rangle. \tag{A 5}$$

Since $\hat{A}_{ij}$ is a solenoidal tensor, it can be decomposed in isotropic MHD as

$$\hat{A}_{ij}(k, t) = P_{ij}(\boldsymbol{k})\frac{A(k, t)}{4\pi k^2} + \mathrm{i}\epsilon_{ijn}\alpha_n\frac{\mathcal{H}^M(\boldsymbol{k}, t)}{k}, \tag{A 6}$$

where $\mathcal{H}^M$ is the true magnetic helicity density, with $k^2\mathcal{H}^M = \mathcal{H}^B$, and $A(k, t)$ is the magnetic potential spectrum, linked to the magnetic energy spectrum $E_B(k, t)$ through

$$A(k, t) = \frac{1}{2}\int_{S_k} \hat{A}_{ii}(\boldsymbol{k}, t)\, \mathrm{d}^2\boldsymbol{k} = k^{-2}E_B(k, t). \tag{A 7}$$

It follows that in the inertial range, the magnetic potential spectrum scales in $A \sim k^{-7/2}$, as obtained in Galtier *et al.* (1999). An evolution equation for $A(k, t)$ could be obtained by spherically averaging the equation of $\hat{A}_{ii}/2$.

A.2. *Residual energy spectrum $E_R(k, t)$*

The emphasis is put here on the residual energy spectrum $E_R = E_V - E_B$. The residual energy spectrum is displayed in figure 11 along with $E_V(k, t)$ and $E_B(k, t)$ for three different initial conditions: in each case $E_B(k, t = 0)$ is given by (2.44), and (*a*) $E_V(k, t = 0) = 0$ with $\sigma_B = 2$, (*b*) $E_V(k, t = 0) = 0$ with $\sigma_B = 4$ and (*c*) $E_V(k, t = 0) = E_B(k, t = 0)$ with $\sigma_V = \sigma_B = 2$. It is revealed that for all three cases, $E_R(k, t)$ is negative, which means that there is an excess of magnetic energy at all scales, and scales in k^{-2} in the inertial range.

Moreover, regarding large scales, one can remark in figure 11 that the infrared scaling of E_R, for wavenumbers smaller than k_L, is either $E_R \sim k^4$, when initially $\sigma_V = \sigma_B$ (simulations not presented here with $\sigma_V = \sigma_B = 1$ and $\sigma_V = \sigma_B = 3$ confirm this observation), or $E_R \sim k^{\sigma_B}$ when $E_V(k, t = 0) = 0$, which is the novelty of this short section.

The k^{-2} inertial scaling of E_R is in agreement with Grappin *et al.* (1983) for imbalanced isotropic MHD, and consistent with Müller & Grappin (2005) for strong MHD with $E_R(k_\perp) \sim k_\perp^{-2}$. In Müller & Grappin (2004), it is argued that the prediction $E_R \sim k^{-2}$ of Grappin *et al.* (1983) stems from non-local considerations, which gives in particular $k^3 E_V^2 \sim k^3 E_B E_R \Rightarrow k^3 E_V^2 \sim k^2 b_0^2 E_R$, where dimensional analysis $kE_B(k) \sim b_0^2$ has been used. Further using the IK scaling (3.2) in the previous equation yields

$$E_R(k, t) \sim \frac{\epsilon}{b_0}k^{-2}. \tag{A 8}$$

This scaling can also be recovered using a method similar to the one of the IK phenomenology. In (3.1), the dissipation rate ϵ can be defined with $u^2 \sim b_0^2$ instead of $u^2 \sim kE$, and $\tau_R = (k^3 E_R)^{-1/2}$ instead of τ_V, so that $\epsilon \sim b_0^2 \tau_A/\tau_R^2 \sim b_0 k^2 E_R$, which
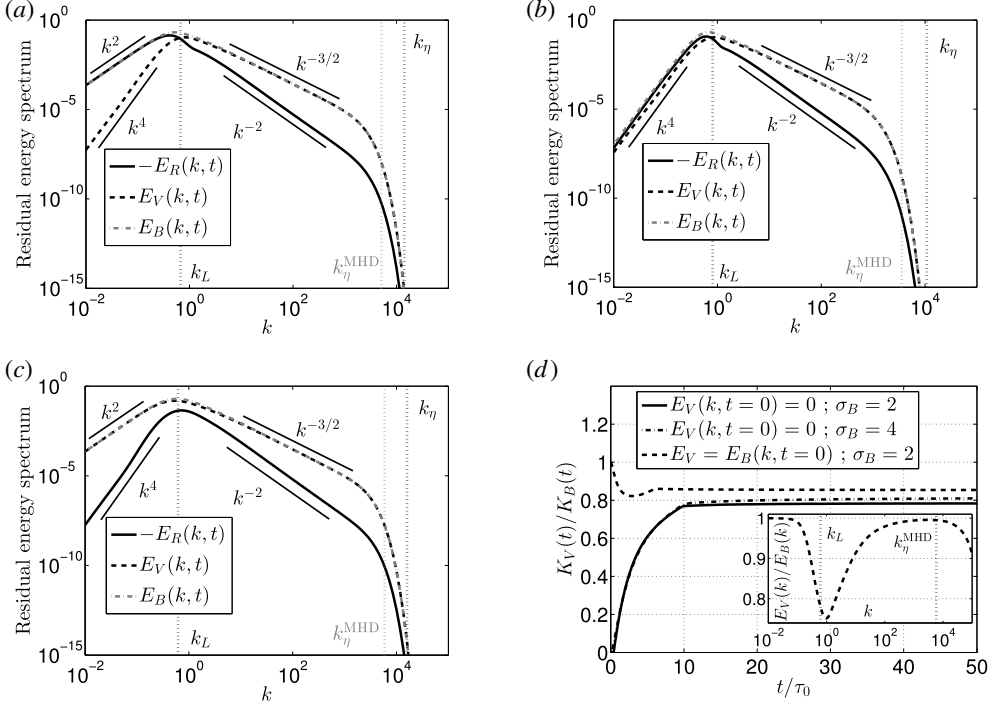
FIGURE 11. Residual energy, kinetic energy and magnetic energy spectra $E_R(k,t)$, $E_V(k,t)$ and $E_B(k,t)$ for various initial conditions, at $Re_\lambda \simeq 2 \times 10^3$, along with the integral, MHD dissipative and Kolmogorov wavenumbers k_L, k_η^{MHD} and k_η. (a) Initial condition (2.44) with $\sigma_B = 2$ and $E_V(k,t=0) = 0$. (b) Initial condition (2.44) with $\sigma_B = 4$ and $E_V(k,t=0) = 0$. (c) Initial condition (2.44) with $E_V(k,t=0) = E_B(k,t=0)$ and $\sigma_V = \sigma_B = 2$. (d) Time evolution of the kinetic to magnetic energy ratio K_V/K_B for the three previous initial conditions; inset is the spectral ratio E_V/E_B for $E_V(k,t=0) = E_B(k,t=0)$ and $\sigma_V = \sigma_B = 2$.

eventually recovers (A 8). The assumption $u^2 \sim kE \to b_0^2$ appears to be appropriate since the difference between the kinetic and magnetic spectra essentially lies at large scales where E_B is stronger than E_V, for various initial conditions, as shown in figure 11. Nevertheless, the k^{-2} inertial scaling for the residual energy spectrum is at odds with the isotropic MHD turbulence results of Müller & Grappin (2004, 2005) where $E_R \sim k^{-7/3}$ is found. This is because in the latter references, the kinetic energy and magnetic energy spectra scale in $E_V \sim E_B \sim k^{-5/3}$, unlike the present simulations where $E_V \sim E_B \sim k^{-3/2}$: using $E_V \sim k^{-5/3}$ in the previous arguments would consistently yield $E_R \sim k^{-7/3}$. Note that the exponents of $E_R^{-m_R}$ and $E^{-m_{\mathrm{tot}}}$ verify the relation $m_R = 2m_{\mathrm{tot}} - 1$ which was recently improved to match solar wind data (Grappin, Müller & Verdini 2016).

In figure 11(d), the kinetic to magnetic energy ratio K_V/K_B is presented for the three previous initial conditions: the asymptotic value of K_V/K_B only slightly depends on initial conditions after a few turnover times τ_0, and in all cases, there is an excess of magnetic energy. In the inset of figure 11(d), the spectral ratio E_V/E_B is presented for the third initial condition, which clearly illustrates that the excess of magnetic energy is mainly localized at large scales.

Finally, the last point to address is the decay of the residual energy $K_R = K_V - K_B$. In figure 4, it is revealed that its decay exponent α_R follows as well the theoretical

predictions (3.6). This is expected, and can be shown in two different ways: (i) writing the continuity of the residual energy spectrum E_R in $k_L = 1/L$ provides

$$k_L^{\sigma-p+2} \sim \frac{\epsilon}{b_0}, \tag{A 9}$$

according to (A 8), which straightforwardly gives $\alpha_R = \alpha$; and (ii) considering the previous characteristic time scale argument giving $\epsilon \sim b_0 u^2/L$, and combining with (3.5), yields again $\alpha_R = \alpha$.

Appendix B. Details on statistics in physical space

In this appendix, some details about the statistics in physical space are provided, first regarding the evolution equations of the total energy K and dissipation rate ϵ, and secondly about the 4/5th law in isotropic balanced MHD turbulence.

B.1. *Evolution equations of K and ϵ*

Some details are first given on the evolution equation of the total energy K. The evolution equations of K_V and K_B read

$$\frac{\partial K_V}{\partial t} = -\epsilon_V + \left\langle u_i b_j \frac{\partial b_i}{\partial x_j} \right\rangle, \quad \frac{\partial K_B}{\partial t} = -\epsilon_B + \left\langle b_i b_j \frac{\partial u_i}{\partial x_j} \right\rangle. \tag{B 1a,b}$$

Since because of homogeneity $\langle u_i b_j \partial_j b_i \rangle = -\langle b_i b_j \partial_j u_i \rangle$, the evolution equation of the total energy K reads

$$\frac{\partial K}{\partial t} = -\epsilon, \tag{B 2}$$

which is similar to the equation for the kinetic energy $K_V(t)$ in HIT. Further identifying with the sum of equations (2.37) and (2.38) integrated over the whole wavenumber space provides

$$\int_0^\infty (S^{\mathrm{V}} + S^{\mathrm{B(mag)}})\, \mathrm{d}k = 0, \quad \int_0^\infty S^{\mathrm{B(mag)}}\mathrm{d}k = -\int_0^\infty S^{\mathrm{V(mag)}}\, \mathrm{d}k = \left\langle b_i b_j \frac{\partial u_i}{\partial x_j} \right\rangle, \tag{B 3a,b}$$

where $\langle b_i b_j \partial_j u_i \rangle$ reflects either the production of energy through the Laplace force, or the stretching of the magnetic field. In can be shown that in fully isotropic turbulence, with simple tensorial arguments as in Pope (2000), one has $\langle b_i b_j \partial_j u_i \rangle = 15 \langle b_1^2 \, \partial_1 u_1 \rangle/2$.

Now, regarding the total energy dissipation rate ϵ. One needs the equations of ϵ_V and ϵ_B, obtained by deriving with respect to x_j the equations (2.1) and (2.2) of u_i and b_i, and using ensemble averages after multiplication by $\partial_j u_i$ and $\partial_j b_i$ respectively. This yields

$$\frac{\partial}{\partial t}\left(\frac{\epsilon_V}{2\nu}\right) + \underbrace{\left\langle \frac{\partial u_i}{\partial x_j} \frac{\partial u_i}{\partial x_l} \frac{\partial u_l}{\partial x_j} \right\rangle}_{(\mathrm{I})} + \underbrace{\left\langle u_l \frac{\partial u_i}{\partial x_j} \frac{\partial^2 u_i}{\partial x_l \partial x_j} \right\rangle}_{(\mathrm{II})}$$

$$= -\underbrace{\left\langle \frac{\partial u_i}{\partial x_j} \frac{\partial^2 p^*}{\partial x_i \partial x_j} \right\rangle}_{(\mathrm{III})} + \underbrace{\left\langle \frac{\partial u_i}{\partial x_j} \frac{\partial b_i}{\partial x_l} \frac{\partial b_l}{\partial x_j} \right\rangle}_{(\mathrm{IV})} + \underbrace{\left\langle b_l \frac{\partial u_i}{\partial x_j} \frac{\partial^2 b_i}{\partial x_l \partial x_j} \right\rangle}_{(\mathrm{V})} + \nu \underbrace{\left\langle \frac{\partial u_i}{\partial x_j} \frac{\partial^3 u_i}{\partial x_j \partial x_l \partial x_l} \right\rangle}_{(\mathrm{VI})},$$

$$(B\,4)$$

$$\frac{\partial}{\partial t}\left(\frac{\epsilon_B}{2\eta}\right) + \underbrace{\left\langle \frac{\partial u_l}{\partial x_j}\frac{\partial b_i}{\partial x_l}\frac{\partial b_i}{\partial x_j}\right\rangle}_{(IV)} + \underbrace{\left\langle u_l\frac{\partial b_i}{\partial x_j}\frac{\partial^2 b_i}{\partial x_l \partial x_j}\right\rangle}_{(II)}$$

$$= \underbrace{\left\langle \frac{\partial u_i}{\partial x_l}\frac{\partial b_i}{\partial x_j}\frac{\partial b_l}{\partial x_j}\right\rangle}_{(IV)} + \underbrace{\left\langle b_l\frac{\partial b_i}{\partial x_j}\frac{\partial^2 u_i}{\partial x_l \partial x_j}\right\rangle}_{(V)} + \eta\underbrace{\left\langle \frac{\partial u_i}{\partial x_j}\frac{\partial^3 u_i}{\partial x_j \partial x_l \partial x_l}\right\rangle}_{(VI)}. \qquad (B\,5)$$

These two equations can be strongly simplified by considering independently the six different groups of terms. First, using homogeneity, incompressibility and classical tensorial algebra given in Pope (2000), one can show that $(I) = 35\langle(\partial_1 u_1)^3\rangle/2$. The two (II) terms are zero because of homogeneity, as found in Betchov (1963) for the one with b_i. The pressure term (III) is zero because of homogeneity as well. The three (IV) terms need further investigation through the sixth-order tensor (B 7). The sum of the two (V) terms is also zero because of homogeneity. Finally, the two (VI) dissipative terms can be written as in (B 6), again because of homogeneity, and one has further $\langle \partial^2_{jl} u_i \, \partial^2_{jl} u_i\rangle = \langle \partial^2_{jj} u_i \, \partial^2_{ll} u_i\rangle$. With these different features, the sum of the two equations yields (B 6).

B.2. *Simplification of the equation for ϵ*

In this part, the evolution equation of the total dissipation rate ϵ in the framework of balanced IMHDT is addressed, in order to simplify its different terms. After some algebra detailed in the previous part, the evolution equation reads

$$\frac{\partial \epsilon}{\partial t} = 2\nu\left(\left\langle \frac{\partial u_i}{\partial x_j}\frac{\partial b_i}{\partial x_l}\frac{\partial b_l}{\partial x_j}\right\rangle - \left\langle \frac{\partial u_i}{\partial x_j}\frac{\partial u_i}{\partial x_l}\frac{\partial u_l}{\partial x_j}\right\rangle\right) - 2\nu^2\left\langle \frac{\partial^2 u_i}{\partial x_l \partial x_l}\frac{\partial^2 u_i}{\partial x_j \partial x_j}\right\rangle$$

$$+ 2\eta\left(\left\langle \frac{\partial u_i}{\partial x_j}\frac{\partial b_i}{\partial x_l}\frac{\partial b_j}{\partial x_l}\right\rangle - \left\langle \frac{\partial u_l}{\partial x_j}\frac{\partial b_i}{\partial x_l}\frac{\partial b_i}{\partial x_j}\right\rangle\right) - 2\eta^2\left\langle \frac{\partial^2 b_i}{\partial x_l \partial x_l}\frac{\partial^2 b_i}{\partial x_j \partial x_j}\right\rangle. \qquad (B\,6)$$

It is well known that the triple velocity correlation is linked to the velocity derivative skewness, and one has $2\langle \partial_j u_i \partial_l u_i \partial_j u_l\rangle = 35\langle(\partial_1 u_1)^3\rangle$. The term in $2\nu^2$ is linked to the so-called palinstrophy, and one has $\langle \partial^2_{jj} u_i \, \partial^2_{ll} u_i\rangle = 35\langle(\partial^2_{11} u_1)^2\rangle$ (Ristorcelli 2006). One can deduce by analogy that the dissipative term in $2\eta^2$ is $\langle \partial^2_{jj} b_i \, \partial^2_{ll} b_i\rangle = 35\langle(\partial^2_{11} b_1)^2\rangle$, which could be called a magnetic palinstrophy.

In what follows, we are interested into the three mixed-derivative kinetic-magnetic correlation terms, more complicated to handle than the triple velocity one. For this purpose, we define the sixth-order tensor

$$H_{ijlnpq} = \left\langle \frac{\partial b_i}{\partial x_n}\frac{\partial b_j}{\partial x_p}\frac{\partial u_l}{\partial x_q}\right\rangle. \qquad (B\,7)$$

In a fully isotropic framework, this tensor has fifteen non-zero components, expressed as products of Kronecker symbols such as $\delta_{ij}\delta_{ln}\delta_{pq}$. Because of symmetries in (B 7), only nine terms are independent:

$$H_{ijlnpq} = c_1\delta_{ij}(\delta_{ln}\delta_{pq} + \delta_{lp}\delta_{nq}) + c_2(\delta_{ip}\delta_{jq}\delta_{ln} + \delta_{iq}\delta_{jn}\delta_{lp}) + c_3\delta_{np}(\delta_{il}\delta_{jq} + \delta_{iq}\delta_{jl})$$

$$+ c_4(\delta_{il}\delta_{jn}\delta_{pq} + \delta_{ip}\delta_{jl}\delta_{nq}) + c_5(\delta_{il}\delta_{jn}\delta_{nq} + \delta_{in}\delta_{jl}\delta_{pq}) + c_6(\delta_{in}\delta_{jq}\delta_{lp} + \delta_{iq}\delta_{jp}\delta_{ln})$$

$$+ c_7 \delta_{in} \delta_{jp} \delta_{lq} + c_8 \delta_{ij} \delta_{lq} \delta_{np} + c_9 \delta_{ip} \delta_{jn} \delta_{jq}. \tag{B 8}$$

The three terms of interest in the equation of ϵ can be expressed as $2\nu H_{ililjj} + 2\eta(H_{ijillj} - H_{iilljj})$. Unlike the term (I) which involves only the velocity field, it is not possible to express all nine constants $c_1, \ldots, c_9$ as functions of one only. Nevertheless, some interesting relations can be found. First, incompressibility provides three equations $2c_1 + 2c_3 + 3c_8 = 0$, $2c_2 + 2c_4 + 3c_9 = 0$ and $2c_5 + 2c_6 + 3c_7 = 0$. Further using homogeneity, one obtains the crucial result $H_{ijljli} = 0$ – which stems from $\langle u_l \partial_j b_i \partial_{il}^2 b_j \rangle = 0$, as already obtained by Betchov (1963) – which gives $15c_8 = 24c_2 + 6c_4 + 4c_5 + 16c_6$. Fortunately, all nine constants are not necessary. Indeed, one gets

$$\left\langle \frac{\partial u_i}{\partial x_j} \frac{\partial b_i}{\partial x_l} \frac{\partial b_j}{\partial x_l} \right\rangle - \left\langle \frac{\partial u_l}{\partial x_j} \frac{\partial b_i}{\partial x_l} \frac{\partial b_i}{\partial x_j} \right\rangle = H_{ijillj} - H_{iilljj} = 30(c_3 - c_1), \tag{B 9}$$

$$\left\langle \frac{\partial u_i}{\partial x_j} \frac{\partial b_i}{\partial x_l} \frac{\partial b_l}{\partial x_j} \right\rangle = H_{ililjj} = 18(c_4 - c_2) + 12(c_5 - c_6). \tag{B 10}$$

The final step is rather tedious and consists into choosing wisely various components of H_{ijlnpq} to determine the remaining constants. It follows that three simple relations can be found, $c_9 = -2\langle \partial_1 u_1 \, \partial_3 b_1 \, \partial_1 b_3 \rangle$, $-2(c_7 + c_8 + c_9) = \langle \partial_1 u_1 \, (\partial_1 b_1)^2 \rangle$ and $2(c_3 - c_1) = \langle \partial_1 u_1 \, (\partial_3 b_1)^2 \rangle - \langle \partial_1 u_1 \, (\partial_1 b_3)^2 \rangle$. Combining all these equations yields the final important results

$$2\nu \left\langle \frac{\partial u_i}{\partial x_j} \frac{\partial b_i}{\partial x_l} \frac{\partial b_l}{\partial x_j} \right\rangle = 30\nu \left[2 \left\langle \frac{\partial u_1}{\partial x_1} \frac{\partial b_1}{\partial x_3} \frac{\partial b_3}{\partial x_1} \right\rangle + \left\langle \frac{\partial u_1}{\partial x_1} \left(\frac{\partial b_1}{\partial x_1} \right)^2 \right\rangle \right], \tag{B 11}$$

$$2\eta \left[\left\langle \frac{\partial u_i}{\partial x_j} \frac{\partial b_i}{\partial x_l} \frac{\partial b_j}{\partial x_l} \right\rangle - \left\langle \frac{\partial u_l}{\partial x_j} \frac{\partial b_i}{\partial x_l} \frac{\partial b_i}{\partial x_j} \right\rangle \right] = 30\eta \left[\left\langle \frac{\partial u_1}{\partial x_1} \left(\frac{\partial b_1}{\partial x_3} \right)^2 \right\rangle - \left\langle \frac{\partial u_1}{\partial x_1} \left(\frac{\partial b_3}{\partial x_1} \right)^2 \right\rangle \right]. \tag{B 12}$$

These two expressions quite simplify the production terms in the equation of the total dissipation rate (B 6).

B.3. *The 4/5th law of isotropic MHD turbulence*

In this section, we investigate further the terms labelled (i) and (ii), which appear in the evolution equation (5.11) of $R + B$. Three two-point third-order correlations are involved, namely

$$\phi_{ijl}^{(uuu)}(r, t) = \langle u_i u_j u_l' \rangle, \quad \phi_{ijl}^{(bbu)}(r, t) = \langle b_i b_j u_l' \rangle, \quad \phi_{ijl}^{(ubb)}(r, t) = \langle u_i b_j b_l' \rangle, \tag{B 13a–c}$$

which are true tensors. The two first ones are symmetric in their two first indices, and thus easier to handle. It appears that using only the evolution equation of R, and thus the term (i), one can recover the 4/5th law of isotropic MHD turbulence (Politano & Pouquet 1998b; Yousef, Rincon & Schekochihin 2007)

$$\langle \delta u_L^3 \rangle - 6\langle b_L^2 u_L' \rangle = -\tfrac{4}{5} r \epsilon, \tag{B 14}$$

as done in Yoshimatsu (2012). The main features of the derivation are recalled here, along with some considerations about the term (ii).

The term (i) depends on $\phi_{ili}^{(uuu)} - \phi_{ili}^{(bbu)}$. After some classical algebra (developed in Politano *et al.* (2003), Briard & Gomez (2017) for instance) these two tensors can be expressed as

$$\phi_{ijl}^{(xxu)}(r, t) = \frac{k_x - rk_x'}{2r^3} r_i r_j r_l - \frac{k_x}{2r} \delta_{ij} r_l + \frac{2k_x + rk_x'}{4r} (\delta_{il} r_j + \delta_{jl} r_i), \quad \text{(B 15)}$$

where the subscript x stands for either u or b, $k_u = \langle u_L^2 u_L' \rangle$, $k_b = \langle b_L^2 u_L' \rangle$ and the prime $'$ on the correlation k_x refers to the spatial derivative $k_x' = \partial_r k_x$. Using homogeneity, one can further show that $k_u = \langle \delta u_L^3 \rangle / 6$. Moreover, from the evolution equations (B 1) of K_V and K_B, it follows that

$$\langle \delta u_i \delta u_i \rangle = 4K_V(t) - 4R(r, t), \quad \frac{\partial K_V}{\partial t} = -\epsilon_V - \epsilon_B - \frac{\partial K_B}{\partial t}. \quad \text{(B 16a,b)}$$

The evolution equation of R thus becomes

$$\frac{\partial}{\partial t} \langle \delta u_i \delta u_i \rangle + 4 \frac{\partial K_B}{\partial t} = -\frac{8\nu}{r^2} \frac{\partial}{\partial r} \left(r^2 \frac{\partial R}{\partial r} \right) - \frac{2}{r^2} \frac{\partial}{\partial r} \left(\frac{1}{r} \frac{\partial}{\partial r} (r^4 (k_u - k_b)) \right) - 4\epsilon. \quad \text{(B 17)}$$

Identification with (5.11) provides

$$\langle \delta u_L \delta u_i \delta u_i \rangle = \frac{1}{3r^3} \frac{\partial}{\partial r} (r^4 \langle \delta u_L^3 \rangle), \quad \langle b_L b_i u_i' \rangle = \frac{1}{2r^3} \frac{\partial}{\partial r} (r^4 \langle b_L^2 u_L' \rangle), \quad \text{(B 18a,b)}$$

where the first of the two relations is usual for HIT. Further dropping the two time derivative and viscous dissipation terms in (B 17), and integrating twice with respect to r yields the 4/5th law (B 14).

Some words can be said about the term (ii) in the equation of $B(r, t)$, which depends on $\phi_{lii}^{(ubb)} - \phi_{ili}^{(ubb)}$. The latter tensor can be expressed as

$$\phi_{ijl}^{(ubb)}(r, t) = \frac{A - B - C - D}{r^3} r_i r_j r_l + \frac{B}{r} \delta_{ij} r_l + \frac{C}{r} \delta_{il} r_j + \frac{D}{r} \delta_{jl} r_i, \quad \text{(B 19)}$$

where $A(r) = \langle u_L b_L b_L' \rangle$, $B(r) = \langle u_N b_N b_L' \rangle$, $C(r) = \langle u_N b_L b_N' \rangle$, $D(r) = \langle u_L b_N b_N' \rangle$, with $A + 2B = 0$ and $C + D = A + rA'/2$, so that $\phi_{iil}^{(ubb)} = 0$, where the subscript $()_N$ refers either to $()_2$ or $()_3$. Expanding (ii) yields

$$\frac{\partial}{\partial r_l} \langle u_l b_i b_i' - u_i b_l b_i' \rangle = \frac{2}{r^2} \frac{\partial}{\partial r} \left(r^2 (D - C) \right), \quad \text{(B 20)}$$

and the quantity $D - C$ can be linked to

$$\langle \delta u_L \delta b_i \delta b_i \rangle - 4 \langle b_L u_i \delta b_i \rangle = 8(D - C), \quad \text{(B 21)}$$

which appears in the calculations of Yoshimatsu (2012). Finally, identification between the latter reference and (5.1) provides an additional relation

$$\langle \delta b_L \delta u_i \delta b_i \rangle = 2 \left(\langle b_L u_i \delta b_i \rangle + \langle b_L b_i \delta u_i \rangle \right). \quad \text{(B 22)}$$

REFERENCES

ALEXAKIS, A. 2013 Large-scale magnetic fields in magnetohydrodynamic turbulence. *Phys. Rev. Lett.* **110** (8), 084502.

ALEXAKIS, A., MININNI, P. D. & POUQUET, A. 2005 Shell-to-shell energy transfer in magnetohydrodynamics. I. Steady state turbulence. *Phys. Rev.* E **72**, 046301.

ANDRÉ, J. C. & LESIEUR, M. 1977 Influence of helicity on the evolution of isotropic turbulence at high Reynolds number. *J. Fluid Mech.* **81**, 187–207.

BAERENZUNG, J., POLITANO, H., PONTY, Y. & POUQUET, A. 2008 Spectral modeling of magnetohydrodynamic turbulent flows. *Phys. Rev.* E **78** (5), 026310.

BANERJEE, R. & JEDAMZIK, K. 2004 Evolution of cosmic magnetic fields: from the very early universe, to recombination, to the present. *Phys. Rev.* D **70**, 123003.

BATCHELOR, G. K. 1950 On the spontaneous magnetic field in a conducting liquid in turbulent motion. *Proc. R. Soc. Lond.* A **201** (1066), 405–416.

BERESNYAK, A. 2011 Spectral slope and kolmogorov constant of MHD turbulence. *Phys. Rev. Lett.* **106** (7), 075001.

BERESNYAK, A. 2014 Spectra of strong magnetohydrodynamic turbulence from high-resolution simulations. *Astrophys. J. Lett.* **784** (2), L20.

BERESNYAK, A. & LAZARIAN, A. 2008 Strong imbalanced turbulence. *Astrophys. J.* **682** (2), 1070.

BETCHOV, R. 1963 A simplified theory of magnetohydrodynamic isotropic turbulence. *J. Fluid Mech.* **17**, 33–51.

BISKAMP, D. 2003 *Magnetohydrodynamic Turbulence*. Cambridge University Press.

BISKAMP, D. & WELTER, H. 1989 Dynamics of decaying two-dimensional magnetohydrodynamic turbulence. *Phys. Fluids* B **1** (10), 1964–1979.

BOLDYREV, S. 2006 Spectrum of magnetohydrodynamic turbulence. *Phys. Rev. Lett.* **96** (11), 115002.

BOLDYREV, S. & PEREZ, J. C. 2009 Spectrum of weak magnetohydrodynamic turbulence. *Phys. Rev. Lett.* **103**, 225001.

BOLDYREV, S., PEREZ, J. C., BOROVSKY, J. E. & PODESTA, J. J. 2011 Spectral scaling laws in magnetohydrodynamics turbulence simulations and in the solar wind. *Astrophys. J. Lett.* **741** (1), L19.

BRIARD, A. & GOMEZ, T. 2017 Dynamics of helicity in homogeneous skew-isotropic turbulence. *J. Fluid Mech.* **821**, 539–581.

BRIARD, A., GOMEZ, T. & CAMBON, C. 2016 Spectral modelling for passive scalar dynamics in homogeneous anisotropic turbulence. *J. Fluid Mech.* **799**, 159–199.

BRIARD, A., GOMEZ, T., SAGAUT, P. & MEMARI, S. 2015 Passive scalar decay laws in isotropic turbulence: Prandtl effects. *J. Fluid Mech.* **784**, 274–303.

BRIARD, A., IYER, M. & GOMEZ, T. 2017 Anisotropic spectral modeling for unstably stratified homogeneous turbulence. *Phys. Rev. Fluids* **2** (4). doi:10.1103/PhysRevFluids.2.044604.

CAMBON, C. & JACQUIN, L. 1989 Spectral approach to non-isotropic turbulence subjected to rotation. *J. Fluid Mech.* **202**, 295–317.

CAMBON, C., MANSOUR, N. N. & GODEFERD, F. S. 1997 Energy transfer in rotating turbulence. *J. Fluid Mech.* **337**, 303–332.

CAMPANELLI, L. 2016 On the self-similarity of nonhelical magnetohydrodynamic turbulence. *Eur. Phys. J.* C **6** (9), 504.

CARATI, D., DEBLIQUY, O., KNAEPEN, B., TEACA, B. & VERMA, M. 2006 Energy transfers in forced mhd turbulence. *J. Turbul.* **7** (51), 1–12.

CHANDRAN, B. D. G. 2008 Strong anisotropic mhd turbulence with cross helicity. *Astrophys. J.* **685** (1), 646.

CHANDRASEKHAR, S. 1951 The invariant theory of isotropic turbulence in magneto-hydrodynamics. *Proc. R. Soc. Lond.* A **204** (1079), 435–449.

DIAMOND, P. H. & BISKAMP, D. 1990 Comments on 'dynamics of decaying two-dimensional magnetohydrodynamic turbulence' [Phys. Fluids B 1, 1964 (1989)]. *Phys. Fluids* B **2** (3), 681–682.

DOBROWOLNY, M., MANGENEY, A. & VELTRI, P. 1980 Fully developed anisotropic hydromagnetic turbulence in interplanetary space. *Phys. Rev. Lett.* **45** (2), 144–147.

FAVIER, B., GODEFERD, F. S., CAMBON, C., DELACHE, A. & BOS, W. J. T. 2011 Quasi-static magnetohydrodynamic turbulence at high Reynolds number. *J. Fluid Mech.* **681**, 434–461.

FRISCH, U., POUQUET, A., LÉORAT, J. & MAZURE, A. 1975 Possibility of an inverse cascade of magnetic helicity in magnetohydrodynamic turbulence. *J. Fluid Mech.* **68**, 769–778.

GALTIER, S. 2009 Wave turbulence in magnetized plasmas. *Nonlinear Process. Geophys.* **16** (1), 83–98.

GALTIER, S. 2016 *Introduction to Modern Magnetohydrodynamics*. Cambridge University Press.

GALTIER, S., POLITANO, H. & POUQUET, A. 1997 Self-similar energy decay in magnetohydrodynamic turbulence. *Phys. Rev. Lett.* **79** (15), 2807–2810.

GALTIER, S., POUQUET, A. & MANGENEY, A. 2005 On spectral scaling laws for incompressible anisotropic magnetohydrodynamic turbulence. *Phys. Plasmas* **12** (9), 092310.

GALTIER, S., ZIENICKE, E., POLITANO, H. & POUQUET, A. 1999 Parametric investigation of self-similar decay laws in MHD turbulent flows. *J. Plasma Phys.* **61** (3), 507–541.

GEORGE, W. K. 1992 The decay of homogeneous isotropic turbulence. *Phys. Fluids* A **7**, 1492–1509.

GOLDREICH, P. & SRIDHAR, S. 1995 Toward a theory of interstellar turbulence. 2: strong Alfvenic turbulence. *Astrophys. J.* **438**, 763–775.

GOMEZ, T., POLITANO, H. & POUQUET, A. 1999 On the validity of a nonlocal approach for mhd turbulence. *Phys. Fluids* **11** (8), 2298–2306.

GRAPPIN, R., FRISCH, U., LÉORAT, J. & POUQUET, A. 1982 Alfvenic fluctuations as asymptotic states of mhd turbulence. *Astron. Astrophys.* **105**, 6–14.

GRAPPIN, R., POUQUET, A. & LÉORAT, J. 1983 Dependence of mhd turbulence spectra on the velocity field-magnetic field correlation. *Astron. Astrophys.* **126**, 51–58.

GRAPPIN, R., MÜLLER, W.-C. & VERDINI, A. 2016 Alfvén-dynamo balance and magnetic excess in magnetohydrodynamic turbulence. *Astron. & Astrophys.* **589**, A131.

HAUGEN, N., BRANDENBURG, A. & DOBLER, W. 2004 High-resolution simulations of nonhelical mhd turbulence. *Astrophys. Space Sci.* **292** (1), 53–60.

HOSSAIN, M., GRAY, P. C., PONTIUS, D. H. JR., MATTHAEUS, W. H. & OUGHTON, S. 1995 Phenomenology for the decay of energy-containing eddies in homogeneous mhd turbulence. *Phys. Fluids* **7** (11), 2886–2904.

IROSHNIKOV, P. S. 1964 Turbulence of a conducting fluid in a strong magnetic field. *Sov. Astron.* **7** (4), 566–571.

KALELKAR, C. & PANDIT, R. 2004 Decay of magnetohydrodynamic turbulence from power-law initial conditions. *Phys. Rev.* E **69**, 046304.

KOLMOGOROV, A. N. 1941 The local structure of turbulence in incompressible viscous fluid for very large Reynolds numbers. *Dokl. Akad. Nauk SSSR* **30**, 301–305.

KRAICHNAN, R. H. 1965 Inertial-range spectrum of hydromagnetic turbulence. *Phys. Fluids* **8** (7), 1385–1387.

KRAICHNAN, R. H. & NAGARAJAN, S. 1967 Growth of turbulent magnetic fields. *Phys. Fluids* **10** (4), 859–870.

LEE, E., BRACHET, M. E., POUQUET, A., MININNI, P. D. & ROSENBERG, D. 2010 Lack of universality in decaying magnetohydrodynamic turbulence. *Phys. Rev.* E **81** (1), 016318.

LÉORAT, J., POUQUET, A. & FRISCH, U. 1981 Fully developed mhd turbulence near critical magnetic Reynolds number. *J. Fluid Mech.* **104**, 419–443.

LESIEUR, M. 2008 *Turbulence in Fluids*, 4th edn. Springer.

LESIEUR, M. & OSSIA, S. 2000 3D isotropic turbulence at very high Reynolds numbers: EDQNM study. *J. Turbul.* **1**, N7.

LESIEUR, M., OSSIA, S. & METAIS, O. 1999 Infrared pressure spectra in two- and three-dimensional isotropic incompressible turbulence. *Phys. Fluids* **11** (6), 1535–1543.

MASON, J., CATTANEO, F. & BOLDYREV, S. 2008 Numerical measurements of the spectrum in magnetohydrodynamic turbulence. *Phys. Rev.* E **77**, 036403.

MATTHAEUS, W. H., POUQUET, A., MININNI, P. D., DMITRUK, P. & BREECH, B. 2008 Rapid alignment of velocity and magnetic field in magnetohydrodynamic turbulence. *Phys. Rev. Lett.* **100**, 085003.

MELDI, M. & SAGAUT, P. 2013*a* Further insights into self-similarity and self-preservation in freely decaying isotropic turbulence. *J. Turbul.* **14**, 24–53.

MELDI, M. & SAGAUT, P. 2013*b* Pressure statistics in self-similar freely decaying isotropic turbulence. *J. Fluid Mech.* **717, R2**, 1–12.

MININNI, P. D. & POUQUET, A. 2007 Energy spectra stemming from interactions of alfven waves and turbulent eddies. *Phys. Rev. Lett.* **99**, 254502.

MÜLLER, W.-C. & BISKAMP, D. 2000 Scaling properties of three-dimensional magnetohydrodynamic turbulence. *Phys. Rev. Lett.* **84** (3), 475–478.

MÜLLER, W.-C., BISKAMP, D. & GRAPPIN, R. 2003 Statistical anisotropy of magnetohydrodynamic turbulence. *Phys. Rev.* E **67**, 066302.

MÜLLER, W.-C. & GRAPPIN, R. 2004 The residual energy in freely decaying magnetohydrodynamic turbulence. *Plasma Phys. Control. Fusion* **46**, B91–B96.

MÜLLER, W.-C. & GRAPPIN, R. 2005 Spectral energy dynamics in magnetohydrodynamic turbulence. *Phys. Rev. Lett.* **95**, 114502.

ORSZAG, S. A. 1970 Analytical theories of turbulence. *J. Fluid Mech.* **41**, 363–386.

PEREZ, J. C. & BOLDYREV, S. 2009 Role of cross-helicity in magnetohydrodynamic turbulence. *Phys. Rev. Lett.* **102**, 025003.

PEREZ, J. C., MASON, J., BOLDYREV, S. & CATTANEO, F. 2012 On the energy spectrum of strong magnetohydrodynamic turbulence. *Phys. Rev.* X **2**, 041005.

POLITANO, H., GOMEZ, T. & POUQUET, A. 2003 von Kármán-Howarth relationship for helical magnetohydrodynamic flows. *Phys. Rev.* E **68**, 026315.

POLITANO, H. & POUQUET, A. 1998*a* Dynamical length scales for turbulent magnetized flows. *Geophys. Res. Lett.* **25** (3), 273–276.

POLITANO, H. & POUQUET, A. 1998*b* von Kàrmàn-Howarth equation for magnetohydrodynamics and its consequences on third-order longitudinal structure and correlation functions. *Phys. Rev.* E **57** (1), R21–R24.

POPE, S. B. 2000 *Turbulent Flows*. Cambridge University Press.

POUQUET, A. 1996 Turbulence, statistics and structures: an introduction. In *Vth European School in Astrophysics*, Lecture Notes in Physics 'Plasma Astrophysics', vol. 468, pp. 163–212. Springer.

POUQUET, A., FRISCH, U. & LÉORAT, J.-L. 1976 Strong mhd helical turbulence and the nonlinear dynamo effect. *J. Fluid Mech.* **77**, 321–354.

RISTORCELLI, J. R. 2006 Passive scalar mixing: analytic study of time scale ratio, variance, and mix rate. *Phys. Fluids* **18**, 075101.

SAGAUT, P. & CAMBON, C. 2008 *Homogeneous Turbulence Dynamics*. Cambridge University Press.

WAN, M., OUGHTON, S., SERVIDIO, S. & MATTHAEUS, W. H. 2012 von Kármán self-preservation hypothesis for magnetohydrodynamic turbulence and its consequences for universality. *J. Fluid Mech.* **697**, 296–315.

YOSHIMATSU, K. 2012 Examination of the four-fifths law for longitudinal third-order moments in incompressible magnetohydrodynamic turbulence in a periodic box. *Phys. Rev.* E **85**, 066313.

YOUSEF, T. A., RINCON, F. & SCHEKOCHIHIN, A. A. 2007 Exact scaling laws and the local structure of isotropic magnetohydrodynamic turbulence. *J. Fluid Mech.* **575**, 111–120.

ZHOU, Y., SCHILLING, O. & GHOSH, S. 2002 Subgrid scale and backscatter model for magnetohydrodynamic turbulence based on closure theory: theoretical formulation. *Phys. Rev.* E **66**, 026309.